NASA TECHNICAL NOTE

NASA TN D-4356

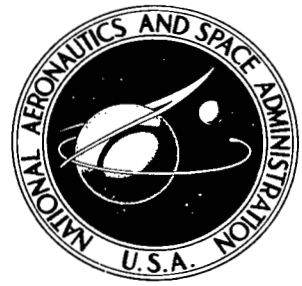

ANALYSIS OF HUMAN RESPONSE IN COMBINED CONTROL TASKS

by Hugh P. Bergeron, James J. Adams, and George J. Hurt, Jr.

Langley Research Center
Langley Station, Hampton, Va.

NATIONAL AERONAUTICS AND SPACE ADMINISTRATION • WASHINGTON, D. C. • MARCH 1968

ANALYSIS OF HUMAN RESPONSE IN COMBINED CONTROL TASKS

By Hugh P. Bergeron, James J. Adams,
and George J. Hurt, Jr.
Langley Research Center

SUMMARY

A study of human-response characteristics in a multitask simulation has been made. The simulation consisted of a primary control task to which were added secondary or side tasks.

A trajectory control problem was used as the primary control task for the pilot. The trajectory task was a fixed-base simulation of a lunar letdown. The task-loading effects on the letdown were found to be predominate during the final hover and translation phase. Therefore, a simplified analytical multiloop representation of this phase of the letdown could be used as the primary control task. All multitask tests were made by using either the lunar-letdown simulation or the multiloop representation as the primary control task. The secondary or side tasks consisted of: (1) a system-failures task integral to a typical space vehicle, and (2) a well-defined motor response task.

The study generated a quantitative index of the information processing characteristics of a full (multitask) simulation. A method for determining the information processing requirements of a trajectory control task was devised to provide the quantity related to this index. By combining this quantity with the information processing measurements of the side tasks, the total workload for various combinations of tasks was determined.

A quantitative analytical model was also generated for the multiloop control in a multitask simulation. A duty-cycle shaping technique developed in this study was used to generate the model.

INTRODUCTION

The optimal use of man in manually controlled missions has always been of the utmost importance in terms of time and cost in the design, fabrication, and utilization of the vehicles involved. Present-day technological advances only amplify this need. Reference 1 discusses the problem in depth. However, work in this area (for example, ref. 2) has generally been concerned only with individual mission problems and usually

cannot be directly related to other missions. What is needed is a better understanding of the intertask relationship inherent to all mission control problems so that solutions of problems of any given mission can be defined and optimized.

The present study is an attempt to identify and define human control in a full (multitask) simulation. The simulation consisted of a primary piloted control task to which were added either one or two side tasks. In the first phase of the study, the primary task was a fixed-base simulation of a lunar-letdown-trajectory control problem. In the second phase of the study, an alternate primary task, a simple multiloop control problem, was used in the multitask simulation. Control of the multiloop system closely approximated control of the final translation and hover phase of the lunar-letdown trajectory, that portion of the letdown trajectory which was most affected by the addition of the side tasks.

The two side tasks were a system-failures task integral to a typical space vehicle and a well-defined motor response task. The system-failures task involved the movement of switches to alternate positions in response to the various failure indications. The motor response task, described in reference 3, consisted of making dots or impacts with a pencil-like device alternately on two separated restricted areas of a small board. Measurements were made of the effects of the side tasks on the time history of the trajectory, the rates at which the system failures were corrected, and the rates at which the dots were made when the tasks were combined. A quantitative measurement, in bits/sec, was obtained of the amount of information processing capacity devoted to the side tasks. This measurement, along with the model of the pilot's response in the trajectory control task, provided a complete description of the pilot's workload in the combined control tasks.

A detailed quantitative analysis was also made with the simpler multiloop representation used for the primary control task by employing a modeling technique described in references 2 and 4 to simulate the pilot's control response in this task. The analytical model was used to describe the pilot's response in the control of the trajectory both with and without the side tasks added; thus, a representation of the changes in pilot response that are brought about by the addition of side tasks was provided.

SYMBOLS

a	center-to-center distance of columns on impact board, inches (centimeters)
B	binary choices, binary digits or bits
b	width of columns on impact board, inches (centimeters)

C	number of responses
G	universal gravitational constant, feet^3/second^2 (meters^3/second^2)
g_E	magnitude of gravitational acceleration at earth's surface, feet/second^2 (meters/second^2)
g_M	magnitude of gravitational acceleration at moon's surface, feet/second^2 (meters/second^2)
h	altitude above moon's surface, feet (meters)
I_{sp}	specific impulse, seconds
i_d	index of difficulty, bits/response
i_p	index of performance, bits/second
K	gain or arbitrary value
K_1,k_1	outer-loop and inner-loop model gain, respectively
K_2,k_2	outer-loop and inner-loop model lead coefficient, respectively, seconds
ℓ	distance from three-dimensional image to vehicle, feet (meters)
ℓ'	perpendicular distance from X'-axis to vehicle, feet (meters)
M	mass of moon, slugs (kilograms)
m	mass of vehicle and fuel at any time, slugs (kilograms)
n_1,n_2,n_3	matrix components of Euler transformation
p,q,r	vehicle rates, radians/second
R	radial distance from vehicle to center of moon, feet (meters)
r_M	radius of moon, feet (meters)

s	Laplace operator, per second
T	thrust, pounds force (newtons)
t	time, seconds
t_{av}	average time, seconds/movement
W	earth weight of vehicle and fuel at any time, pounds force (newtons)
W_o	initial earth weight of vehicle and fuel, pounds force (newtons)
X,Y,Z	image reference axes
X',Y',Z'	image body axes
x',y',z'	distances measured along X', Y', and Z' axes from vehicle to image, feet (meters)
X_B,Y_B,Z_B	vehicle body axes
X_I,Y_I,Z_I	vehicle reference axes
α	transformation angle of three-dimensional image about X-axis, radians
β	transformation angle of three-dimensional image about Z'-axis, radians
γ	central angle, radians
δ	stick displacement (for pitch, roll, or yaw)
θ,ϕ,ψ	Euler angles, radians
τ	model-lag frequency-break point, radians/second
dt	differential with respect to time, per second

A single dot over a symbol denotes a derivative with respect to time. Double dots over a symbol denote a second derivative.

TASKS

A description of the analog representation and of the equipment used in presenting the lunar-letdown-trajectory control task is given. Also, the equipment and procedure used in presenting the simplified representation of the trajectory task (i.e., the multiloop task) and the two side tasks are described.

Lunar-Letdown-Trajectory Control Task

The closed-loop, or primary, control task in the first phase of the study was a lunar descent maneuver initiated from a circular orbit and resulting in near-zero horizontal and vertical velocities at a predefined hover altitude. The equations of motion are given in appendix A. The descent was usually initiated in automatic mode. During this automatic-descent sequence, the pilot could, if he so desired, take over control and manually fly the vehicle by controlling attitude and thrust magnitude in an attempt either to follow the same profile defined for the automatic descent or to deviate from it as he saw fit. Pilot control was exercised from inside the capsule of a procedures trainer that was originally used in the Mercury program. Figure 1 shows the capsule, the operator's console, and the necessary power supplies of the procedures trainer.

In automatic mode, the letdown was initiated from a 50 000-foot (15 240-meter) circular orbit. The vehicle was oriented such that it was braking, with maximum thrust, in the direction of horizontal translation until at a predetermined time the vehicle was pitched down with thrust oriented 20^{o} from the local horizontal. This pitch attitude was maintained until a near-zero horizontal and vertical velocity was reached. At that point either the maneuver was terminated or the pilot took over manually and established a hover condition. During some maneuvers it was necessary for the pilot to take over early in the trajectory so as to correct a programed malfunction. Some typical malfunctions were either high or low thrust, misalined pitch and/or thrust, and attitude damper failures. Since the pilot could expect these failures, he was required to monitor those instruments from which he could determine if the letdown was following the desired profile. For example, the eight ball could be used as a good partial check on the descent profile through the entire letdown trajectory. All the other instruments could be used for accurate checks at certain points in the trajectory. The altimeter and clock, for example, could be used for an accurate check on the profile 1 minute after the start of the maneuver, at the 20^{o} pitchdown point, and at hover.

The altimeter was a single-needle dial instrument on which the complete 320^{o} span of the dial movement represented 50 000 feet (15 240 meters) until the 5000-foot (1524-meter) point was reached. Below this point a change was automatically made in the scaling such that the 320^{o} span represented the final 5000 feet (1524 meters). A

zero-center-scale microammeter was used as a horizontal-velocity indicator. Zero horizontal velocity was indicated when the needle was centered. The meter deflection was proportional to the horizontal velocity up to the maximum meter reading, which indicated a horizontal velocity of 570 ft/sec (174 m/sec). A fully deflected meter could also represent a velocity in excess of 570 ft/sec (174 m/sec). The direction of the deflection indicated the direction of vehicle translation along the X_I-axis. This instrument gave the pilot a crude estimation of the horizontal travel, the accuracy being comparable with that he could obtain by looking out a window. A fuel meter gave the percentage of fuel remaining. The position of the thrust lever also gave the pilot a general idea of the amount of thrust he was commanding. This information was helpful in obtaining and maintaining the hover condition. The thrust was throttlable from 100 percent to a minimum of 10 percent.

Another source of information on vehicle position and attitude was a simulated window. The window was represented by a mirror and was located as depicted in figure 2. The out-the-window viewing area covered a 90° solid angle with the center of the window alined with the X-axis. The viewing angle of the mirror, which represented the window, was only a 20° solid angle. Using the mirror would be the same as scaling down all motion outside the window by a factor of 4.5. The small mirror was used because of the size and layout of the procedures trainer. The apparent viewing area, that which is encompassed by a 90° solid angle, was chosen because it roughly approximated the viewing area of one configuration of the Lunar Module (LM) window.

A target reference with no horizon or background was positioned downrange of the desired landing site. A light spot on an x-y plotter was used as the downrange viewing reference in the initial maneuvers. The light spot would move up and down or side to side with any translation or attitude change of the letdown vehicle. Figure 3 shows a typical record of the target location in the out-the-window view. In latter maneuvers, a three-dimensional conical shape generated by an electronic image generator and reproduced on an oscilloscope was used to replace the light spot.

It was believed that the three-dimensional cone would add to the realism of the out-the-window view. The cone allowed a differentiation to be made between vehicle attitude and translational changes. The cone was located on the surface of the moon and would appear to grow in size as the vehicle approached it. It was not defined to be any particular object, but it could be used, as would a rock formation or other object on the surface, to visually detect and interpret motion of the control vehicle. The image, as produced on the oscilloscope, was relayed to the subject via closed-circuit television. Figure 4 shows the cone located to the left-front and below the control vehicle. An x-y plotter or television monitor, depending on which system was being used, was mounted at the rear of the pilot's head and viewed in the mirror placed in front of him (see fig. 2).

The image generator and the closed-circuit television system used in producing and displaying the three-dimensional cone are shown in figure 5. The equations required to orient the cone are described in appendix B. The Euler transformation required to position the target (cone or light spot) is presented in appendix A. This transformation is the same as that used to orient the simulated vehicle.

The attitude of the vehicle was controlled by the sidearm controller integral to the Mercury procedures trainer. A small dead band was inserted in the output of the controller to compensate for the hysteresis effects of control-stick friction. For maximum stick deflection, the dynamics of the system produced a maximum angular acceleration of $8^{o}/sec^{2}$, a maximum angular velocity of $8^{o}/sec$, and a theoretical unlimited rotation capability. These values are in the range suggested for the LM. When the rate feedback signal is taken out (the equivalent of a damper failure), the theoretical maximum angular velocity also becomes unlimited. The attitude control created pure couples and the translational thrust was assumed to be directed through the center of gravity. The center of gravity is always considered to be the center of the vehicle-reference-axis system. The mass of the fuel required for attitude control was not considered in the computations. Neither was the change in vehicle rotational dynamics due to the change in the vehicle mass brought about by fuel usage in the main engine.

Translation was accomplished by the appropriate rotation of the vehicle and thrust vector. The thrust-mass ratio was 12.88 ft/sec^{2} (3.92 m/sec^{2}) initially, with the total mass of vehicle and main-engine fuel being 26 250/32.2 slugs – that is, 815 slugs (11 890 kilograms). As the fuel mass decreased, the thrust-mass ratio correspondingly increased. The comparable value of T/W, which was 0.4 at the beginning of the letdown, increased to a value of 0.827 at the point of no fuel. A specific impulse of 310 seconds was used.

Multiloop Control Task

The multiloop simulation represents a system which is supported by a thrust alined along the vertical body axis, and translation is obtained by changing the attitude of the vehicle to obtain the desired horizontal component of thrust. The system is therefore similar to that represented in the more complete lunar-letdown simulation, but is restricted to only horizontal translation. In references 2 and 4, the inner-loop control variable (attitude angle) was represented by an angle on a meter mounted on the x-y plotter. In the present multiloop task, the simulated vehicle attitude was controlled by the pitch axis of the sidearm controller, but was displayed as a vertical displacement on an x-y plotter. This positive or negative vertical displacement served as the input used to control the horizontal displacement. Figure 6(a) is a block diagram of the piloted simulation, and figure 6(b) is the corresponding analytical representation. The

sidearm-controller output in pitch was scaled to ±10 volts. This output was used with a dynamics of $K/s(s + 1)$ to control the vertical displacement on the x-y plotter. This vertical displacement was used with a dynamics of K/s^2 to control the horizontal displacement on the plotter. The sensitivities of the vertical and horizontal displacements on the x-y plotter were 10 v/in.

The control task was to translate back and forth between two points located on a horizontal center line, with a hover maintained at each point for a specified time. The pilot controlled this task from inside the capsule of the procedures trainer. An x-y plotter was mounted at the rear of the pilot's head, and a mirror placed in front of him was used to present the display. This setup is the same as that shown in figure 2.

Vehicle-System-Failures Task

A modified Mercury procedures trainer was used as the simulator. The life-support and electrical systems and the failure capabilities integral to the trainer were ideally suited for a system-failures task. The system failures that were used herein were categorized and then listed in several quasi-random lists. (For a more explicit explanation of these system failures and their sequence, see appendix C.) The lists were then used to present vehicle-system failures to the pilot. The failures were administered as rapidly as the operator could present them relative to the response of the subject. In the early tests, no record was made of the exact time each failure was given or corrected, nor was a record taken of piloting mistakes made in correcting the failures. However, this information was obtained in later tests. Data from both sets of tests are considered.

Motor Response Task

The motor response task was used to better define the amount of time consumed in conducting the other tasks. It was ideal for this purpose because of its completely self-pacing quality. Also, it did not directly interfere with the performance of the other tasks and therefore could be used effectively as a fill-in task. The task consisted of placing dots (impacts) alternately on two columns. An impact board with two metal strips mounted side by side for the columns was used, as shown in the following sketch:

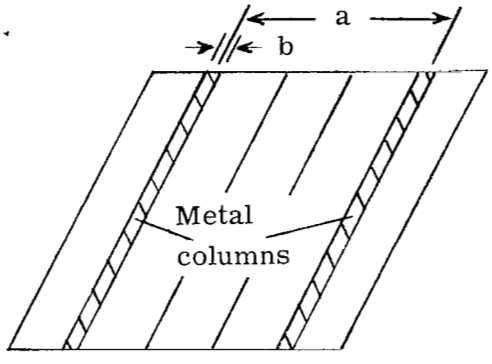

A strap was attached to the board so that it could be mounted on the subject's left leg, just above the knee, as is shown in figure 7. A metal-tipped stylus weighing approximately 1 ounce (0.278 newton) and about the size of a pencil was used to make the dots or impacts. When the stylus made contact with the metal strip, an electrical circuit was closed. This information was recorded on a chart recorder. The columns were 0.25 inch (0.635 cm) wide and were placed 4 inches (10.16 cm) apart center-to-center. A theory has been hypothesized for determining the workload or performance index for this task in bits/sec. Reference 3 gives a detailed explanation of this theory and defines the index of difficulty for the task to be $i_d = -\log_2 \frac{b}{2a}$ bits/response (in the notation of the present paper). Therefore, the performance index would be $i_p = -\frac{1}{t_{av}} \log_2 \frac{b}{2a}$ bits/sec where t_{av} is the average time in sec/movement. It should be emphasized that even though the theory is based on information processing, the numerical values of i_p obtained for this task should only be used as a relative measure when compared with values for other separate and entirely different tasks.

In the present experiment, no documentation was made of the number of undershoot and overshoot impacts. A permanent time history was recorded, however, of the impacts on the assigned columns, and thus direct comparisons of the various tasks could be made to determine the effect of one on the other.

The impact board was mounted on the left leg of the subject and his left hand was used to position the stylus. The instructions were: "Strike the plates alternately and refrain from sliding the stylus point across the plates or board. The number of hits will determine the scoring." A raised area 1.5 inches (3.81 cm) wide was placed in between the two metal strips to discourage sliding of the stylus.

RESULTS

Time histories of manually controlled maneuvers obtained for the various combinations of trajectory control and side tasks with experienced subjects, and the analytical representations of some of these maneuvers, are presented in figures 8 to 19.

Lunar-Letdown Trajectory

Figure 8 is a record of the lunar-letdown maneuver with nominally correct control inputs being made automatically. The corresponding control observed for the lunar-letdown maneuver performed by an experienced National Aeronautics and Space Administration test pilot is shown in figure 9. Of particular significance in these maneuvers are the altitude and vertical-velocity traces. As can be seen for the manually controlled maneuver, the vertical velocity does not have any large variations and therefore the altitude trace is correspondingly smooth, down to and through the hover period. The

instrumentation for this maneuver consisted of an eight ball, an altimeter, and a horizontal-velocity meter. An out-the-window display presented by using the x-y plotter was also employed as a visual cue. Attitude control was obtained through a sidearm controller, and vehicle translation was obtained from the main-engine thrust lever, with thrust vectored as a function of the vehicle attitude. Figure 9 indicates that this instrumentation was sufficient for carrying out the task successfully.

If the difficulty of the lunar-letdown control task is increased by degrading the control dynamics, the deterioration of the maneuvers appears to be minor. An example is presented in figure 10 for a maneuver in which all three attitude controls had damper failures. However, if the pilot workload is increased by adding a side task, the deterioration is significant. Figure 11 illustrates the effect of adding the system-failures task (see appendix C) to the primary control task. The failure sequence for this test began 3 minutes after the start of the primary control task (it had been previously determined that the failures had little effect on the first part of the maneuver). The portion of the letdown up to the point where the final pitchover maneuver was initiated (at $t \approx 5$ minutes) remained unchanged, but from the beginning of the final pitchover maneuver throughout the hover portion, significant variations were observed in the vertical velocity. The result on the hover altitude is a variation of as much as ±2000 feet (±610 meters).

It is interesting to note that the pilot generally considered the control problem due to attitude damper failures (see fig. 10) more difficult than the addition of the system-failures task (see fig. 11). Combining the system-failures task with a test in which the attitude controls had damper failure resulted in a compounding of the effects previously noted (see fig. 12).

In several tests, significant variations were also detected in the horizontal velocity near the point where the final pitchover maneuver was initiated. These variations are directly related to the altitude characteristics at that point inasmuch as the transition to hover was accomplished in a two-step procedure. The altitude and horizontal-velocity control inputs were made separately rather than at the same time and thus a smooth transition of both maneuvers at the same time was improbable. This type of control was occasionally detected in the tests with no system failures, but not nearly as often as in tests with failures.

Multiloop Trajectory

It would have been desirable to use a mathematical model of the pilot to reproduce the lunar-letdown maneuver so as to obtain an analytical expression for the letdown control loop, but the direct application of an analytical model to this maneuver was beyond the scope of the present study. However, references 2 and 4 present a method by which an analytical model was applied to a simplified multiloop simulation. This simulation

was similar to the end portion of the altitude trace of the lunar letdown in figure 8 of the present paper – that portion which was affected most by the addition of the side tasks. The multiloop simulation and the lunar letdown are alike in that both simulations use a change in one mode of control to obtain a change in a second mode. The inner loop in the multiloop simulation is directly comparable to vehicle attitude in the lunar letdown and the outer loop is directly comparable to the altitude.

The piloted multiloop simulation was conducted from inside the Mercury procedures trainer with the display presented in the same manner as the out-the-window display of the lunar letdown. Figure 13(a) presents a typical manually controlled multiloop maneuver in which there were no side tasks. Figure 13(b) is an analytical representation of this manually controlled maneuver. Constant gains were used in the model of this analytical representation. As can be seen, a very good match was obtained for the outer-loop control and a fairly good match, for the inner-loop control. The primary difference in the results for the inner-loop control appeared as a difference in the amplitude of the higher frequency control outputs. The complete closed-loop characteristics of the multiloop simulation with the model in the loop (fig. 13(b)) included an inner-loop frequency of 1.11 rad/sec with a damping ratio of 0.046. An overly damped frequency characteristic of the outer loop of about 0.2 rad/sec (that is, a 30-second period) was also produced.

The system-failures task was added to the multiloop trajectory control task in the same manner that it was added to the lunar-letdown task. When the system-failures task was added to any task, several results were observed. In general, the pilot's correction times were longer than for the system-failures task when performed alone, the amount of increase in time depending on the effort put into or the difficulty of the primary task. In addition, the output of the primary task also showed detrimental effects. For example, the effect of adding failures to the multiloop control task produced a degradation in both output modes of that task, as shown in figure 14(a). The end portion of the inner-loop output no longer shows the smooth characteristics observed in figure 13(a). The variations of the inner loop also resulted in a variable, low-frequency oscillation in the outer-loop output which was similar to the variation in altitude observed for the lunar letdown in figure 11.

A second side task, a motor response task, was tried in conjunction with the multiloop simulation. This particular task did not have any direct association with a realistic mission control situation, but it did have the advantage of being directly measurable in the unit bits/sec. The motor response task was first performed by itself to obtain a relative workload rate. It was found that the subjects (all using the left hand) would obtain a fairly consistent rate for the operation of the task alone. For the pilots of the majority of the tests discussed, this rate turned out to be an i_p of 8.7 bits/sec.

When the motor response task was added to the piloted multiloop control task (see fig. 15), it was observed that the degradation of the multiloop task was similar to that when the system-failures task was the secondary task (see fig. 14(a)). The measured i_p for the motor response task performed during the test in figure 15 was 4.1 bits/sec.

An attempt was made to duplicate the pilot's control of the multiloop task in a combined-task situation by utilizing a mathematical model in the multiloop task (refs. 2 and 4). The ability of a constant-coefficient linear model to reproduce the time history of the manually controlled trajectory has been shown in figure 13. However, this model would not reproduce the trajectory obtained for the combined tasks without some modification. The modification to this constant-coefficient model which produced the best results was the inclusion of an on/off duty cycle for the outer-loop lead coefficient. The lead coefficient was switched off as a function of the outer-loop output being within a preselected error band for a specific length of time. The time interval that produced the best results was that time required for three control peaks to occur. The "off" time, which can be considered as a function of the workload of a secondary task, was selected so as to reproduce the closed-loop characteristics of the manual maneuvers. At the end of this "off" time, the translation would again be tested and the switch on the lead coefficient again cycled. A high-speed, repetitive-operation analog computer was used in these tests. The computer used digital logic to count the control peaks. Limiters and comparators were used to construct the error-band criteria. The method produces a time history like that shown in figure 14(b). The logic can be interpreted, in the manually controlled simulation, as the pilot's controlling the translation maneuver so as to place it in a predefined area and then assuming that it would, with only indirect attention, stay there for a length of time. This time could then be utilized in performing some other task(s), after which he would return full attention to the multiloop control task, realine the translation portion of the simulation, and repeat the cycle.

The on/off switching of the parameter K_2 in the end portion of the multiloop simulation with system failures added is shown in figure 14(b). The "off" time for this simulation was set at 11 seconds. This value represents an "off" time for the lead coefficient K_2 of about 60 percent of that portion of the maneuver in which "off" times were incorporated. The maximum amount of "off" time which would still cause no noticeable change in response was about 7 seconds, or about 40 percent "off" time.

Figures 14(a) and 14(b) show a remarkable degree of similarity in both the end portion of the attitude (inner-loop output) trace and in translation (outer-loop output). However, the first two large outputs of the inner loop in figure 14(b) do not show the randomness exhibited in the first portion of the piloted maneuvers. A better match of

this portion of the inner-loop output was obtained by using a similar on/off switching logic. In this logic the inner-loop gain k_1 was switched on and off. This switching was done as a function of the number of peaks specified for the inner-loop output to remain within a selected band. This band had been determined from an examination of previous piloted maneuvers. A typical result from this arrangement is presented in figure 14(c). The occurrence of flat areas in the region of the two inner-loop control limits is the primary characteristic of this technique. The interpretation of this logic applied to the manually controlled maneuvers involves the assumption that the pilot tends to look away or disregard for a time the inner-loop control once a predetermined error criterion has been met. Then, after a calculated length of time, control is returned to the inner loop, and any necessary adjustment or change is made, after which the cycle is repeated. This refinement does not contradict but rather adds to the previously mentioned logic for the end portion of the multiloop task. It should be noted that the gain-change modifications to either the outer-loop or inner-loop pilot representations (that is, reducing the gains to zero) could not be allowed during the very critical time when the large changes in attitude occurred. To do so would have delayed the inner-loop crossover through zero. This crossover point is very critical and is usually monitored fairly accurately by the subjects, even when performing an additional side task.

The inner-loop lead coefficient k_2 could also have been switched on and off to represent the pilot's control. However, the resulting ramp-like outputs were not considered to be as representative of the piloted maneuvers as the flat regions which were produced when the inner-loop gain k_1 was used.

It was realized that a simple reduction in the outer-loop model lead coefficient K_2 would bring about a long-period, poorly damped oscillation of the outer-loop output similar to that obtained in the piloted maneuvers. This reduction, however, also produced a low-frequency, quasi-sinusoidal output in the attitude (inner-loop output). This type of modification was therefore given no further consideration.

Another method which had shown some initial promise of improving the model response was a simple switching logic used to switch the outer-loop model lead coefficient K_2 on and off at some preset frequency, with the actual on/off times also fixed. The problem encountered with this particular technique was that the preset on/off times would not necessarily coincide with good control techniques. At times the control input would be switched off when large errors existed. Also, the on/off times could produce a time-phase relationship that would lead to a divergence. Figure 16 is a typical example of such a maneuver.

A switching of the outer-loop gain K_1 was also attempted, both with the simple preset switching logic and with the error-criterion switching logic. Neither switching

technique provided the desired match of the piloted maneuvers. The predominant result was a large variation in the inner-loop output, with small but sharp reversals in the outer-loop output.

Representation of Side Tasks

A general quantitative representation was used to describe the side or secondary tasks. For the motor response task this representation was a measure of performance in bits/sec. The average rate for the subjects, all using the left hand, was 8.7 bits/sec when this task was performed alone. When combined with the trajectory control task, if no degradation was observed in the trajectory task, the motor-response-task rate decreased to 3 bits/sec. If the subject attempted to increase the motor-response-task rate beyond this point, the effect was a degradation of control in the trajectory task. The change in the trajectory task became definitely evident when the motor-response-task rate reached 4 bits/sec. These values in bits/sec for the motor response task were obtained by averaging the results of six maneuvers each for five trained subjects. A typical example of the trajectory time history, when the processing rate on the motor response task was 4.1 bits/sec, is given in figure 15. A similar degradation of the trajectory task was reproduced analytically in figure 14(b) by incorporating analytical pilot models and by using a switching logic on the outer-loop parameter K_2. This time history of the piloted trajectory was reproduced by using an "off" time of 11 seconds. For this example the average switching frequency that resulted was 0.0526 hertz.

A measure of the performance of the system-failures task in bits/sec was obtained by considering the number of possible responses for each failure. This number ranged from two to as many as eight, with an overall average of about four. By using the formula for binary choices $B = \log_2 C$, where C is the number of responses and B is bits, the average information content was found to be about 2 bits/failure. A typical example of a failure indication is the fan-motor failure. It requires one of five possible corrective actions: fuse, fan-motor, inverter, main-battery, or standby-battery corrective response.

A complete failure sequence of 21 failures, when performed alone, took approximately 200 seconds to complete, the rate averaging out to 1 bit every 4.75 seconds. The sequence was then run in conjunction with the trajectory task. The total time, and therefore the rate based on this time, did not change. However, it was observed that the measured time from an individual failure onset to the corrective response did change. Therefore, the number of bits/failures was related to this correction time. However, the processing rate based on the individual correction times was still quite low. For example, when the task was done alone, the failures were corrected in 2 to 3 seconds on the average, and when the task was done in conjunction with the trajectory control task

such that it affected the trajectory, the correction times averaged 3 to 6 seconds. Therefore, the indicated rate of processing determined on this basis was still a low value of 0.33 to 1 bit/sec.

In an attempt to gain a better insight on the processing rate for the system-failures task, it was compared with the rate for the motor response task. The assumption was made that when the two tasks were performed together, their processing rates could be added linearly and the sum would equal the rate at which the motor response task was performed alone. The results for a test in which the two tasks were performed together are shown in table I under test F. The motor response task had a measured processing rate of 4.0 bits/sec in this test. According to the assumption that was made, the failure task was being performed at 4.7 bits/sec.

It was further assumed that the processing rate for the system-failures task was a function of the previously mentioned measured correction times. In analyzing the data and comparing these correction times, it was observed that failures which were identical except for the required physical movement differed by a constant time factor which could be related to the physical-movement time. Therefore, it is proposed that part of the time required to correct the failures can be attributed to a physical-movement time of the subjects which does not vary as the workload is increased. This time turns out to be approximately 0.7 second for the system failures used in this report. Consequently, the times used to determine the processing rate were refined to the extent that they were now the actual correction times minus the physical-movement time. These refined times were considered to be an inverse function of the processing rate for the system-failures task.

The indication is that some function of the correction time would be a useful variable in describing the workload of any task for which this time is available. This indication would suggest the use of logically obtained specified correction times to determine the workload of proposed side tasks. By using the measured correction times of this system-failures task of the present study, it was determined that when the subject performed the system-failures task alone, the workload was 5.7 bits/sec $\left(\text{that is, } \frac{2.54}{2.1} = \frac{i_p}{4.7}\right.$ and hence $\left. i_p = 5.7 \text{ bits/sec}\right)$. The value of 5.7 bits/sec is in general agreement with the observed fact that the failure task did not constitute a 100 percent workload by itself because some time was required on the part of the experimenter to set up each new failure.

In order to further check the validity of this method for determining the workload of the failures task, tests were made in which the subject was required to handle all three tasks – the trajectory control task, the motor response task, and the system-failures task – simultaneously. In order for this method to be applied, the trajectory

task had to be given a similar workload measure. Thus, the motor response task and the trajectory control task were performed together, and the linear sum of the two workloads was assumed to equal the processing rate for the motor response task performed alone. Several experimental points were used to establish the relation. One was the point where the subjects could perform the motor response task with no effect observed on the trajectory control. The motor-response-task rate for this point was 3 bits/sec. With more and more emphasis being placed on the motor response task in succeeding tests, additional points with the motor-response-task rate at 4, 4.5, 5.25, and 7.6 bits/sec were obtained. These experimental points were used to establish a subjective rating in bits/sec based on the precision of control of the trajectory task. Deviations in both the inner-loop and outer-loop outputs from the steady-state value were weighted to determine the ratings of the workload measurements. These ratings for the trajectory control task, the measured correction times mentioned previously for the system-failures task, and the values of i_p for the motor response task were used to obtain the total workload. It was believed that a reasonably good description for the failures task had been made if the sum of the processing rates for all three tasks as performed in a single test equaled 8.7 bits/sec.

The results from some typical tests are shown in figures 17 to 19 and presented in table I. Figures 17, 18, and 19 correspond to tests B, E, and G, respectively, in table I. The results in table I show that the total workload in tests G, H, I, and J is only slightly less than the expected 8.7 bits/sec. It is therefore concluded that the technique of comparing a complex task, such as the failures task, with a simple task, such as a motor response task, can be used to establish a useful representation of the workload for the complex task. It was also shown that the technique can be extended to other types of tasks as exemplified by the results for the trajectory task. However, extreme caution must be observed in choosing the side task to be used as the basis of workload measurement. This task must not interact with, such as to interfere with or add to, the task with which it is being performed.

The fact that the total workload was consistently under the expected rate of 8.7 bits/sec could be due to several factors, the most obvious being that the transition times might be significant. However, without going deeper into the experiment, it would appear that the fairly simple techniques employed in this report can produce data which are accurate enough to be used in many present-day workload studies. A more detailed analysis which would include the aforementioned and other, now apparent, factors should produce a refinement of the data.

CONCLUDING REMARKS

Quantitative measurements were made to determine the characteristics and workloads of several tasks both when performed alone and when combined. Relative values were obtained for the workload requirements of three separate tasks: a trajectory control task, a system-failures task, and a motor response task. The workload relationships of one to another were determined when the tasks were performed together.

The study showed that combining a manually controlled multiloop trajectory control task with side tasks causes a deterioration in the precision of the control of the trajectory. It was further shown that this deterioration can be reproduced by suitable modification of the constant-coefficient linear models used to represent the pilot's control. The principal modification was the inclusion of an on/off duty cycle for the outer-loop lead coefficient of the model. An additional refinement was achieved by also including a simular duty cycle for the inner-loop model gain.

The methods and techniques used in this study can be useful in analyzing and characterizing realistic control tasks to determine their best man-machine integration relationship. Trade-offs between precision of trajectory control and the amount of information processing capacity devoted to side tasks could be determined and would be applicable for most multitask simulations.

Langley Research Center,
National Aeronautics and Space Administration,
Langley Station, Hampton, Va., October 11, 1967,
125-19-01-09-23.

APPENDIX A

EQUATIONS USED IN LUNAR-LETDOWN SIMULATION

Equations of Motion

The translation equations of motion used in the lunar-letdown simulation were those for a point source mass moving in a planar force field. The equations are

$$\ddot{R} = R(\dot{\gamma})^2 + \frac{T}{m} n_2 - \frac{GM}{R^2} \tag{1}$$

$$\ddot{\gamma} = \frac{\frac{T}{m} n_1 - 2\dot{R}\dot{\gamma}}{R} \tag{2}$$

$$\ddot{Z}_I = \frac{T}{m} n_3 \tag{3}$$

The Z_I-axis translation was part of the control problem even though it was not considered in the orbital computations. The last term in equation (1) can be simplified to

$$\frac{GM}{R^2} \approx g_M \left(\frac{r_M}{R}\right)^2$$

as long as $R - r_M$ is relatively small. Also,

$$g_M \left(\frac{r_M}{R}\right)^2 \approx g_M + Kh$$

where K is a small number (-1.84×10^{-6}) which gives the best linear approximation. Thus, equation (1) becomes

$$\ddot{R} = R\dot{\gamma}^2 + \frac{T}{m} n_2 - g_M - Kh$$

Also,

$$W = W_o - \int_0^t \dot{W}\, dt$$

with

$$\dot{W} = \frac{T}{I_{sp}}$$

and

$$W = mg_E$$

APPENDIX A

A diagram showing the axis-system orientation is presented in the following sketch:

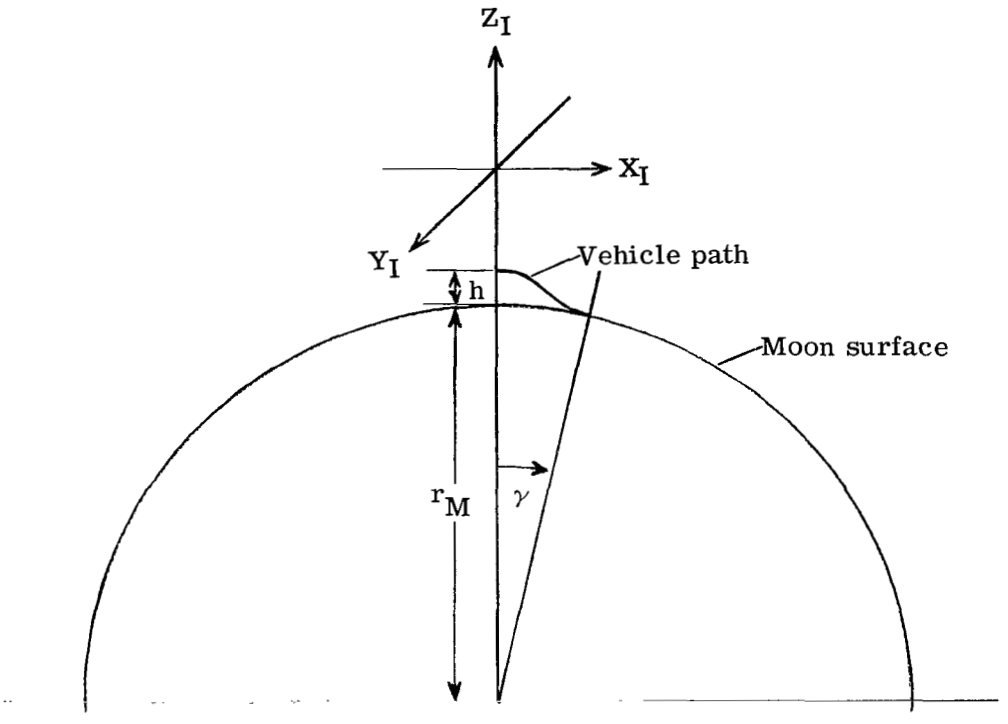

Since the central angle γ transversed during descent did not change greatly, the resultant change in vehicle attitude from the local horizontal, due to this angle change, was not determined (i.e., the surface of the moon was considered flat).

Attitude Equations

The attitude equations were written in transfer-function form and were scaled to provide a maximum angular acceleration of $8^o/sec^2$ and a maximum angular velocity of $8^o/sec$. The three equations are

$$\frac{p}{\delta} = \frac{K}{s+1}$$

$$\frac{q}{\delta} = \frac{K}{s+1}$$

$$\frac{r}{\delta} = \frac{K}{s+1}$$

APPENDIX A

Euler Angle Transformation

The Euler angle transformation used was a yaw-pitch-roll transformation. The rate transformation is

$$\dot{\phi} = p + \dot{\psi} \sin \theta$$

$$\dot{\theta} = q \cos \phi - r \sin \phi$$

$$\dot{\psi} = \frac{r \cos \phi + q \sin \phi}{\cos \theta}$$

and the axis transformation is

$$\begin{bmatrix} \cos \psi \cos \theta & \sin \psi \cos \theta & -\sin \theta \\ \cos \psi \sin \theta \sin \phi - \sin \psi \cos \phi & \cos \psi \cos \phi + \sin \psi \sin \theta \sin \phi & \cos \theta \sin \phi \\ \cos \psi \sin \theta \cos \phi + \sin \psi \sin \phi & \sin \psi \sin \theta \cos \phi - \cos \psi \sin \phi & \cos \theta \cos \phi \end{bmatrix} \begin{bmatrix} X_I \\ Y_I \\ Z_I \end{bmatrix} = \begin{bmatrix} X_B \\ Y_B \\ Z_B \end{bmatrix}$$

where

$$\cos \psi \sin \theta \cos \phi + \sin \psi \sin \phi = n_1$$

$$\sin \psi \sin \theta \cos \phi - \cos \psi \sin \phi = n_2$$

$$\cos \theta \cos \phi = n_3$$

Since it was necessary to pitch the vehicle more than 90^o and since a 90^o pitch angle produced a singularity point, a 90^o roll angle was inserted for the initial or zero condition. As a result, the yaw and pitch motions on the eight ball were switched and also the vector relation of the body and inertial axes changed to $Y_B = Z_I$, $Z_B = -Y_I$, and $X_B = X_I$ for the initial condition. The resultant axis transformation was used to vector the thrust in the orbital equations. The axis transformation was also used to position the target in a simulated window area. This positioning was accomplished by dividing the horizontal and vertical body-axis distances by the distance to the target.

APPENDIX B

THREE-DIMENSIONAL ELECTRONIC IMAGE GENERATOR

An electronic image generator (fig. 5) was used to produce the three-dimensional conical shape (fig. 4) employed in the lunar-letdown simulation. The image generator utilized only two axes of rotation, but because of the symmetry of the image in the third axis an apparent three degrees of rotational freedom of the cone could be obtained. The cone was also capable of three degrees of translational freedom.

The image generator required that the inputs for rotation be the sine and cosine functions of the two required rotations. Translation was obtained by using the appropriate voltages corresponding to the translational displacements.

Derivation of Angular Transformation

The cone is considered to be in the axis system depicted in the following sketch:

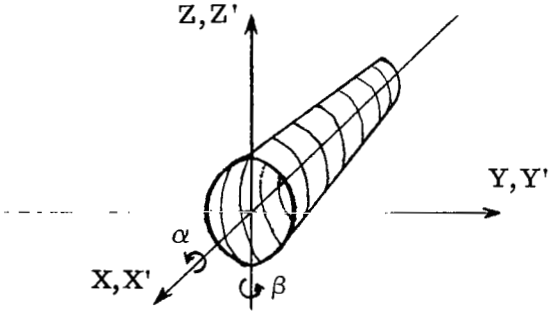

The angle α is always a rotation around the X image reference axis, and the angle β is a rotation around the Z' image body axis. It should be noted that the axis of symmetry is a rotation around the X' image body axis. The cone can be oriented such that it appears to be an object in space, about which one can move, by employing the equations derived in this appendix with the use of the following sketch:

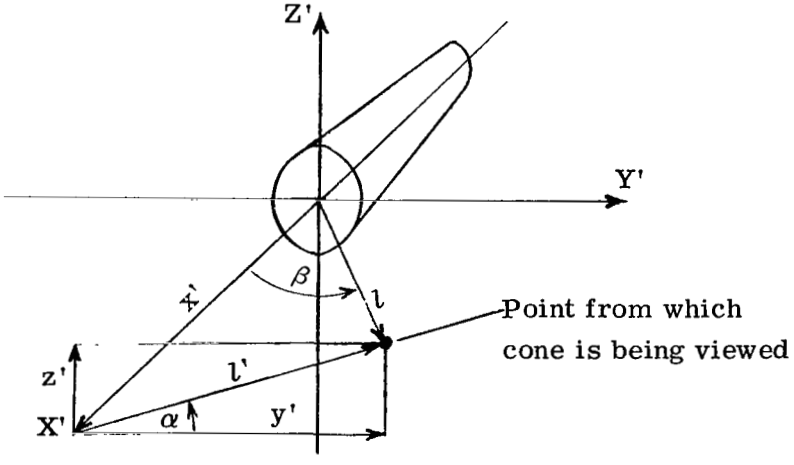

APPENDIX B

With x', y', and z' being the distances measured along the X'-, Y'-, and Z'-axes from the viewing point to the image,

$$l' = \sqrt{(y')^2 + (z')^2}$$

and

$$\alpha = \sin^{-1} \frac{z'}{\sqrt{(y')^2 + (z')^2}}$$

That is,

$$\sin \alpha = \frac{z'}{l'}$$

and

$$\cos \alpha = \frac{y'}{l'}$$

Also,

$$l = \sqrt{(l')^2 + (x')^2}$$

and

$$\beta = \sin^{-1} \frac{l'}{\sqrt{(l')^2 + (x')^2}}$$

That is,

$$\sin \beta = \frac{l'}{l}$$

and

$$\cos \beta = \frac{x'}{l}$$

The angle α must also include the inertial axis roll generated when rotating the viewing vehicle.

These computations can be obtained by polar resolution. The computer diagram for this technique is shown on the next page. In this diagram l is the distance to the image and is therefore used to vary the size of the image. Up-down and side-to-side translations of the image are obtained by the appropriate inertial axis transformation in pitch and yaw (from appendix A) in conjunction with the inertial displacements.

It should be noted that the aforementioned formulas for orienting the three-dimensional cone have two singularity points. The first one is when both y' and z' equal zero. Then, $\cos \alpha$ and $\sin \alpha$ both equal 0/0, which is indeterminate. No great problem would result, however, when using a polar resolution on an analog computer to generate α and l', since if y' or z' were equal to zero where the other went through zero, there would only be an instantaneous 180° change in the angle at the

APPENDIX B

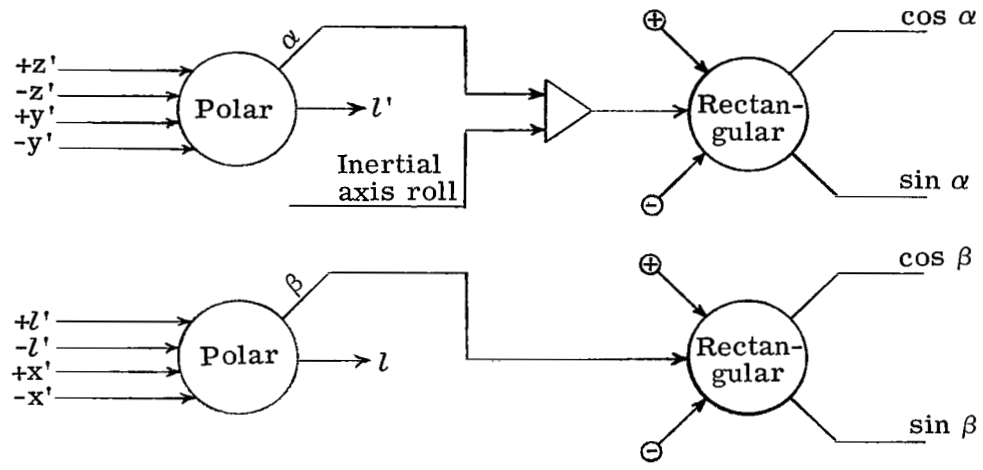

zero-zero condition such that the object would be correctly oriented after emergence from this zero-zero condition. The instantaneous 180^{o} change would produce a visual flicker or jerk of the image but would not overload the computer or cause the simulation to be stopped inasmuch as the image would still be in its correct aspect.

The other singularity point is a compounding of the first. It exists when all three distances equal zero – that is, when x', y', and z' equal zero. When this condition occurs, not only do $\cos \alpha$ and $\sin \alpha$ equal 0/0, but also $\cos \beta$ and $\sin \beta$ equal 0/0. If this situation were to exist, then the cone would have to be at the same place in space as the viewing point – obviously, an unlikely occurrence.

APPENDIX C

SYSTEM-FAILURES TASK

The system failures were obtained from those systems present in the Mercury procedures trainer. However, because of the different requirements of the present simulation, several of the systems could not be used. With the systems chosen, several lists of quasi-random arrangements were formed. These lists were then used to present the system failures to the test subjects. A typical list of failures, the corresponding indications, and the required responses is presented in this appendix. It can be noted that several responses are required for certain failures because of the hierarchy of response predetermined for particular failure indications. This hierarchy of response was necessary since several failures generated the same indication.

Failure	Indication	Response
1. CO_2	Slow increase in reading of CO_2 partial pressure meter	Reach with left hand and pull decompression lever; after 2 to 3 seconds, return decompression lever and pull recompression lever; after 2 to 3 seconds, return recompression lever and make verbal notification of decompression to experimenter
2. Normal suit fan	Fan motor stops; dc ammeter drops from 20 to 15 amperes	Switch to no. 2 suit-fan fuse and then switch to no. 1 suit fan
3. Automatic-stabilization-and-control-systems inverter	Standby-inverter automatic warning light comes on	Switch standby-inverter automatic tone switch off
4. No. 1 standby battery	None yet	None yet
5. No. 2 standby battery	(See no. 4); dome temperature warning light and out-of-orbit-mode warning light go off	Switch standby battery to on position
6. No. 1 pitch fuse	When pitch control not used, verbal indication from experimenter only	Switch to no. 2 pitch fuse
	When pitch control used, indication is no response from the stick in pitch	Switch to no. 2 pitch fuse
7. No. 2 suit-fan fuse	Fan motor stops; dc ammeter drops from 20 to 15 amperes	Switch to no. 1 suit-fan fuse
8. Fan inverter	Light dims, then returns to normal; ac voltmeter decreases, then returns to normal	None yet
9. All main batteries	Apparent failure of the following components: Fan motor, cabin lights, right side of control fuel meter, dc voltmeter, dc ammeter, ac voltmeter, eight ball, emergency O_2 meter, partial-pressure meter, suit-environment meter, and out-of-orbit-mode warning light	Switch ammeter to bypass; switch ammeter back to normal; since standby-battery switch already on, switch isolated battery to standby position
10. No. 2 suit-fan fuse returned to operation	None yet	None yet
11. No. 1 yaw fuse	When yaw control not used, verbal indication from experimenter only	Switch to no. 2 yaw fuse
	When yaw control used, indication is no response from the stick in yaw	Switch to no. 2 yaw fuse
12. ac voltmeter	Loose ac voltmeter	Verbal response to experimenter
13. Main and standby batteries returned to normal operation	Verbal indication from experimenter	Switch isolated battery to normal and switch standby battery to off

APPENDIX C

Failure	Indication	Response
14. Automatic transfer of standby inverter	(See no. 3); eight ball tumbles; (see no. 8); fan motor stops; cabin lights go off; failure of ac voltmeter; dc ammeter drops from 20 to 8 amperes	Switch fan inverter to standby
15. No. 1 suit fuse	Fan motor stops; dc ammeter drops from 20 to 15 amperes	Switch to no. 2 suit fuse (see no. 10)
16. 3-volt power	Apparent failure of the following components: Right side of control fuel meter; emergency O_2 meter, suit-environment meter, and partial-pressure meter	Switch to 3-volt supply
17. Normal suit fan returned to operation	None yet	None yet
18. dc power	Same indication as for no. 9 (partial-pressure meter is already failed (see no. 16))	Switch ammeter to bypass (ammeter stays failed)
19. Automatic-stabilization-and-control-systems inverter returned to operation	None (see no. 14)	None
20. dc voltmeter	Failure of dc voltmeter	Verbal response to experimenter
21. All main batteries	Same indication as for no. 9 (partial-pressure meter is already failed (see nos. 16 and 18)); ammeter is already failed (see no. 18)	Since ammeter already switched to bypass (see no. 18), switch standby battery to on position
22. Fan inverter returned to normal	None yet	None yet
23. No. 1 suit fan	Fan motor stops	Switch to no. 1 suit fuse, next switch to normal suit fan, and then switch to no. 2 suit fuse (see nos. 15 and 17)
24. Standby inverter	Fan motor stops; cabin lights go off; ac voltmeter fails	Switch fan inverter to normal
25. No. 1 roll fuse	When roll control not used, verbal indication from experimenter only	Switch to no. 2 roll fuse
	When roll control used, indication is no response from stick in roll	Switch to no. 2 roll fuse
26. Nos. 1 and 2 standby batteries	Same indication as for no. 21	Since ammeter already switched to bypass (see no. 18) and standby battery already switched on (see no. 21), switch isolated battery to standby
27. Normal suit fan	Fan motor stops	Switch to no. 1 suit fuse, next switch to no. 1 suit fan, then switch to no. 2 suit fuse, and finally switch to no. 2 suit fan

REFERENCES

1. Fitts, Paul M.: Functions of Man in Complex Systems. Aerospace Eng., vol. 21, no. 1, Jan. 1962, pp. 34-39.

2. Bergeron, Hugh P.; Kincaid, Joseph K.; and Adams, James J.: Measured Human Transfer Functions in Simulated Single-Degree-of-Freedom Nonlinear Control Systems. NASA TN D-2569, 1965.

3. Fitts, Paul M.: The Information Capacity of the Human Motor System in Controlling the Amplitude of Movement. J. Exptl. Psychol., vol. 47, no. 6, June 1954, pp. 381-391.

4. Adams, James J.; Bergeron, Hugh P.; and Hurt, George J., Jr.: Human Transfer Functions in Multi-Axis and Multi-Loop Control Systems. NASA TN D-3305, 1966.

TABLE I.- WORKLOAD RESULTS FOR TYPICAL TESTS

Test	Task emphasis	Average correction time of failures, sec	Average workload, bits/sec			
			System failures	Motor response	Trajectory	Total
A – Motor response only				8.7		8.7
B – Trajectory only					5.0	[a]5.0
C – Failures only		2.1	5.7			[a]5.7
D – Motor response and trajectory	Trajectory			4.8	[b]3.9	8.7
E – Motor response and trajectory	Motor response			7.8	[b].9	8.7
F – Motor response and failures	Failures	2.54	[b]4.7	4.0		8.7
G – Trajectory and failures	Failures	2.34	5.1		3.2	[c]8.3
H – Trajectory and failures	Trajectory	4.26	2.8		4.2	[c]7.0
I – Motor response, trajectory, and failures	Motor response	6.28	1.9	5.4	1.2	[c]8.5
J – Motor response, trajectory, and failures	Trajectory	5.43	2.2	2.7	3.2	[c]8.1

[a]Obtained from extrapolation of task from known values.

[b]Obtained from comparing with motor response task.

[c]Obtained from summation of individual task values.

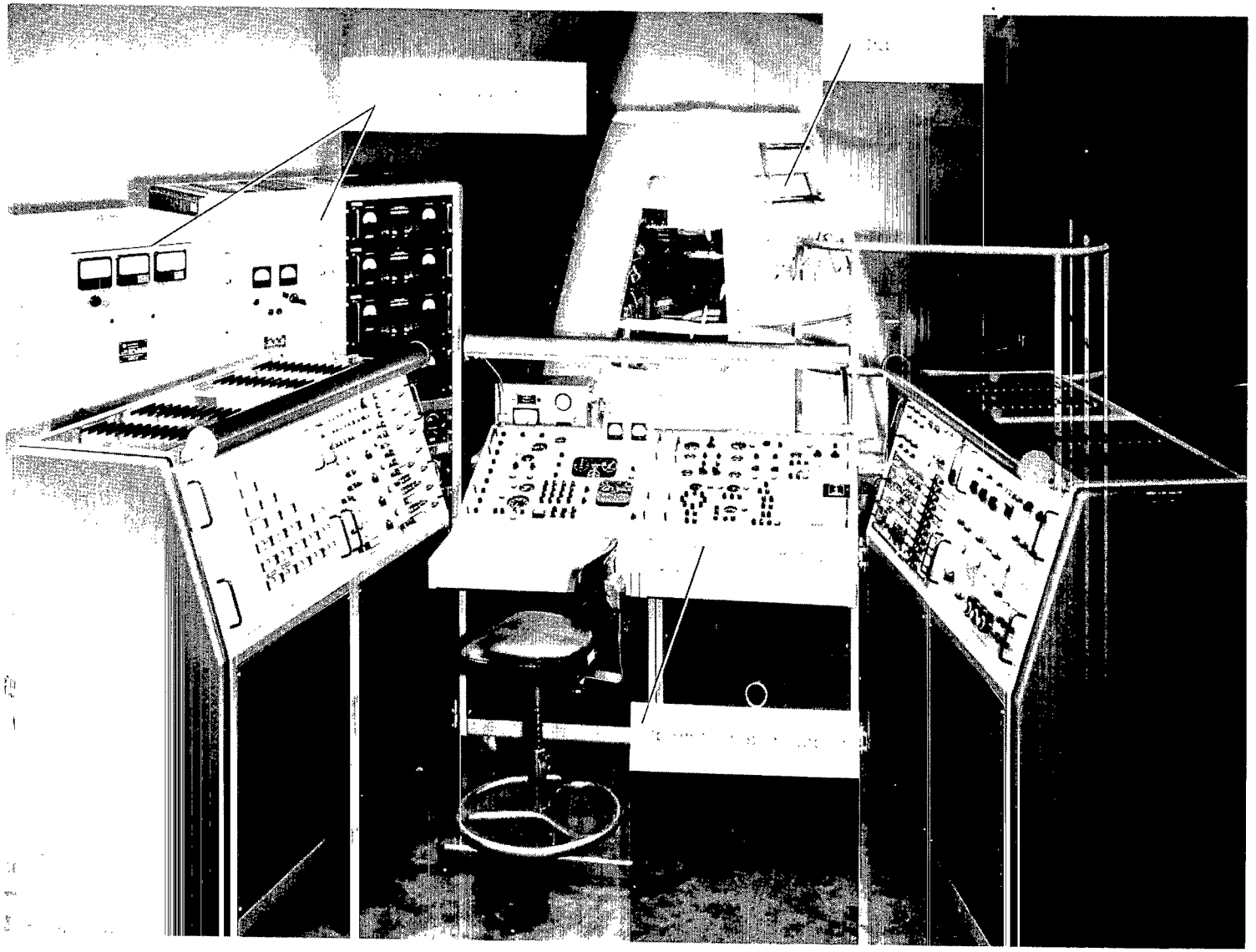

Figure 1.- Mercury procedures trainer and its associated equipment.

L-64-2603.1

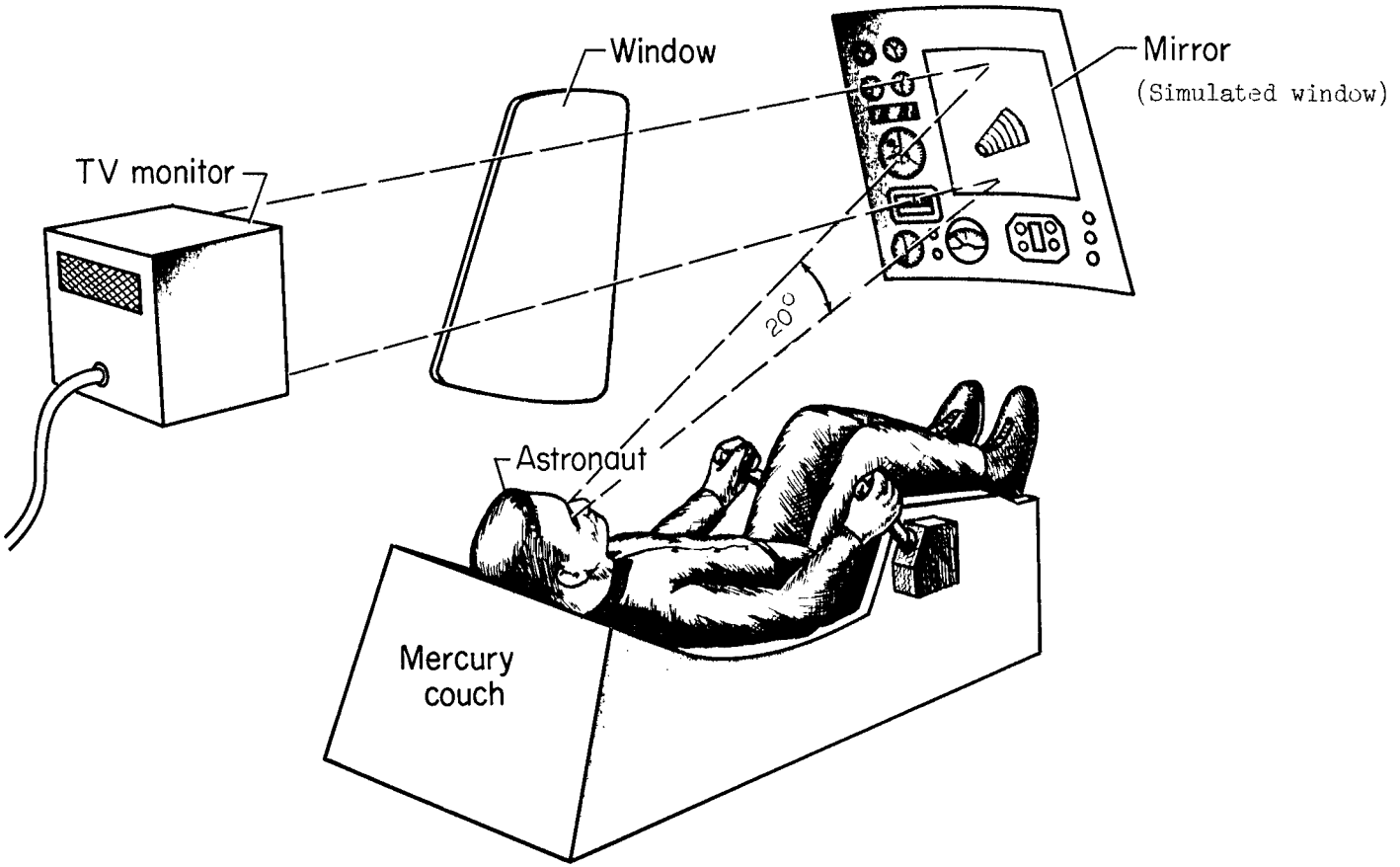

Figure 2.- Simulated-window configuration used in lunar-letdown and multiloop tasks.

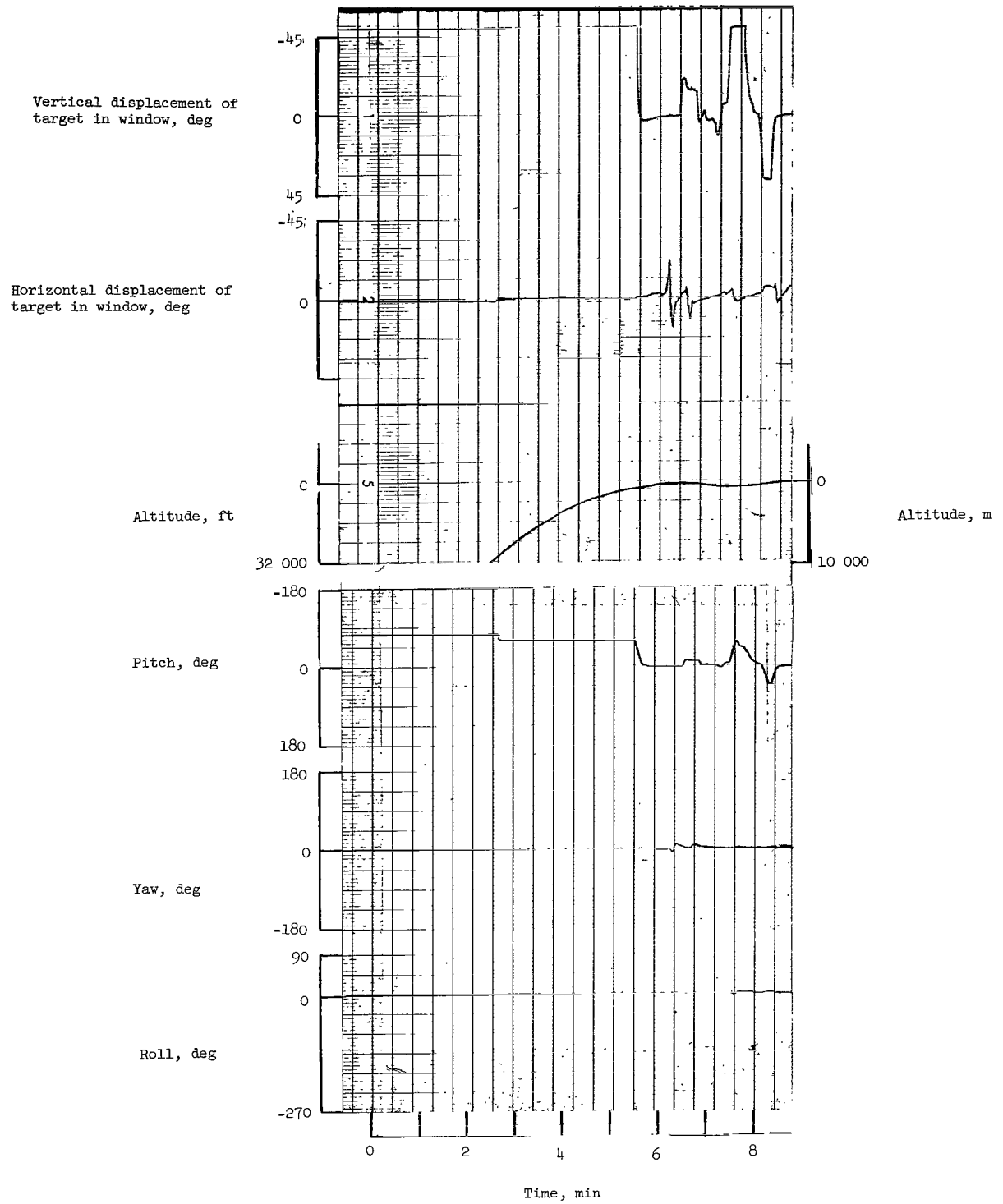

Figure 3.- Typical record of image location in out-the-window view.

Figure 4.- Photograph of three-dimensional cone as seen by the subject. L-67-6699

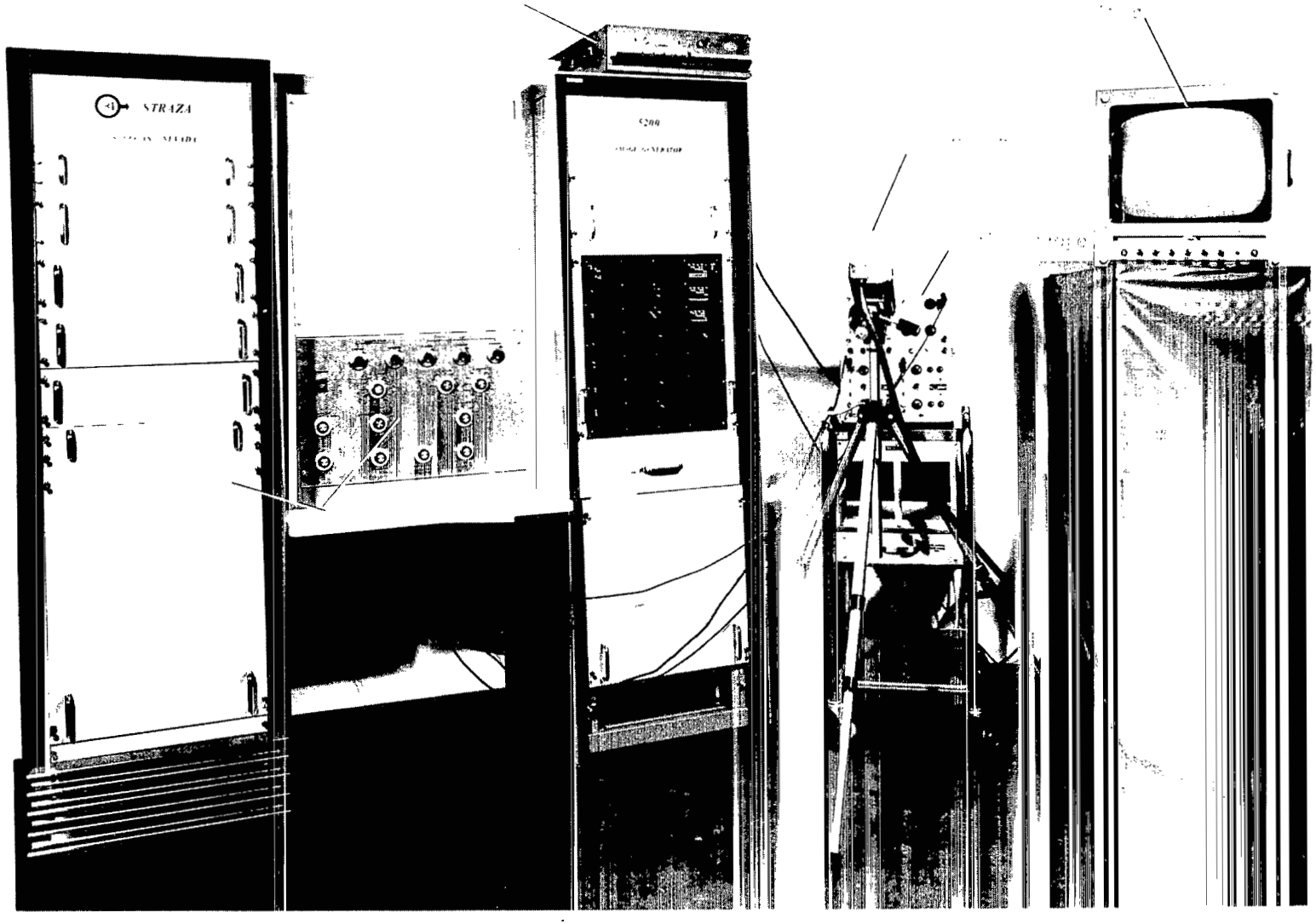

Figure 5.- Image generator and closed-circuit television system used in displaying the three-dimensional cone. L-65-7077.1

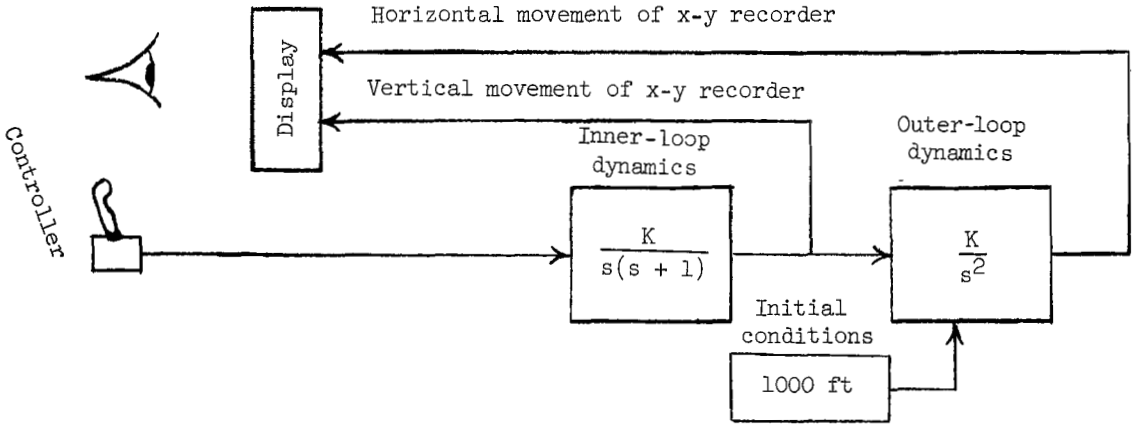

(a) Piloted simulation.

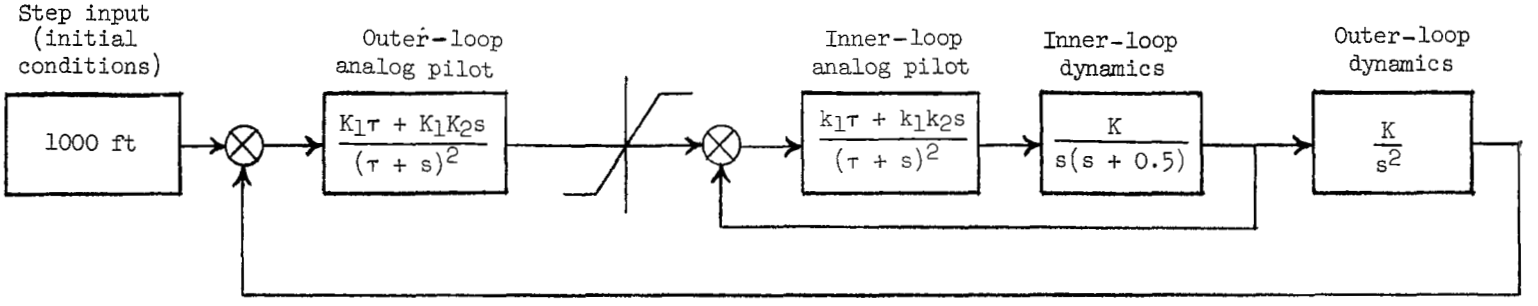

(b) Analytical representation.

Figure 6.- Block diagrams of multiloop simulation.

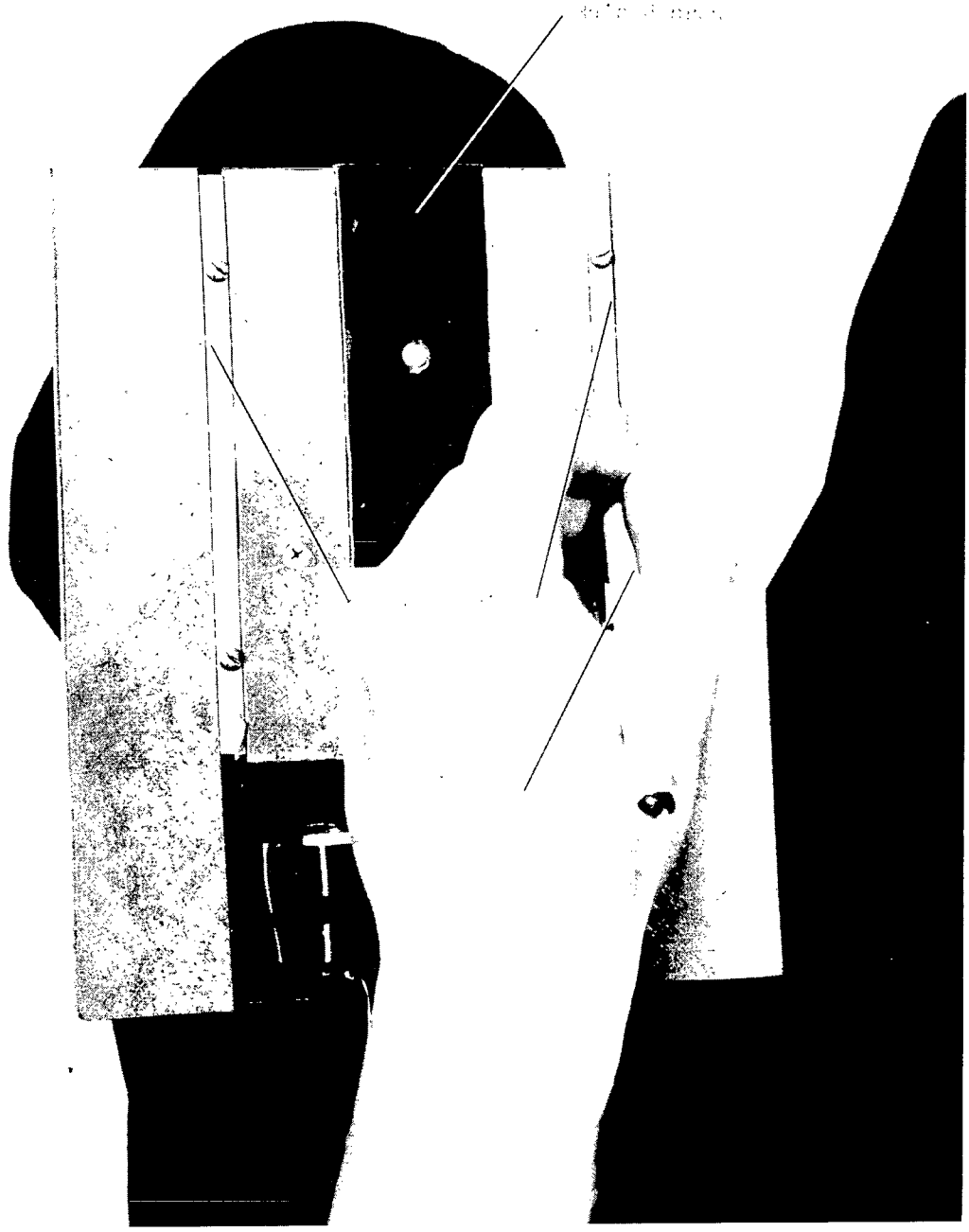

Figure 7.- Impact board used in motor response task. L-66-5051.1

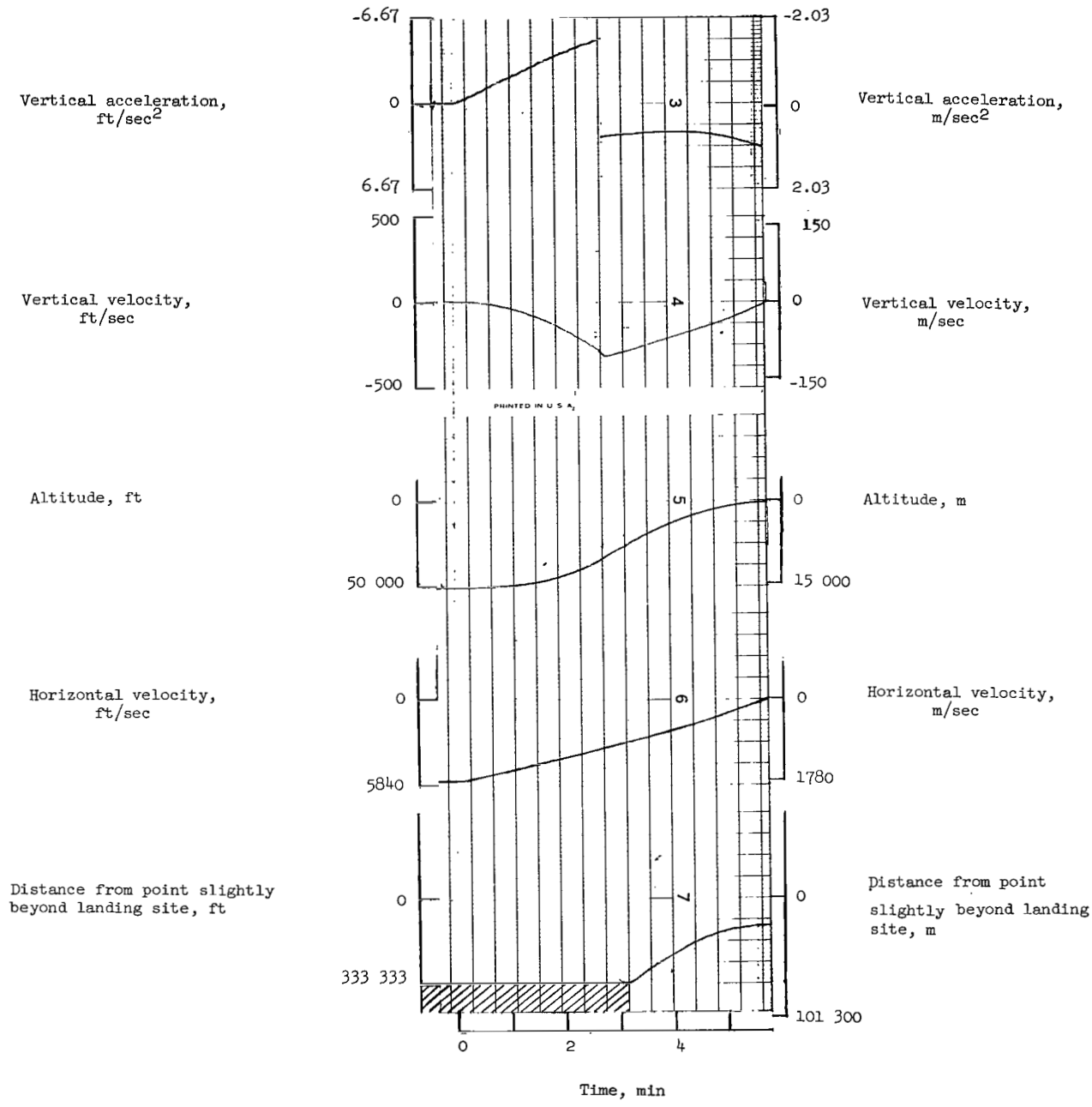

Figure 8.- Lunar-letdown maneuver in automatic mode.

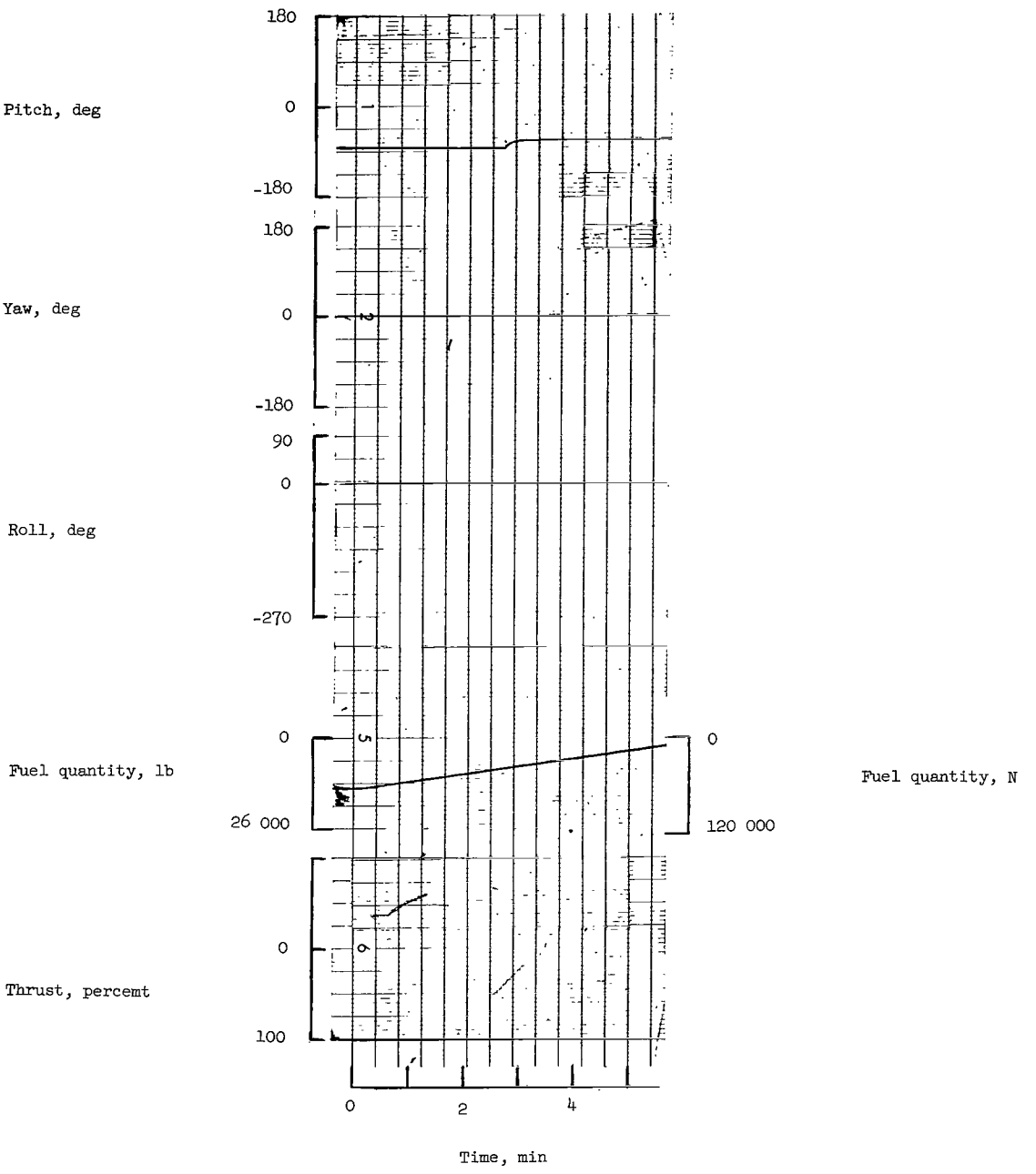

Figure 8.- Concluded.

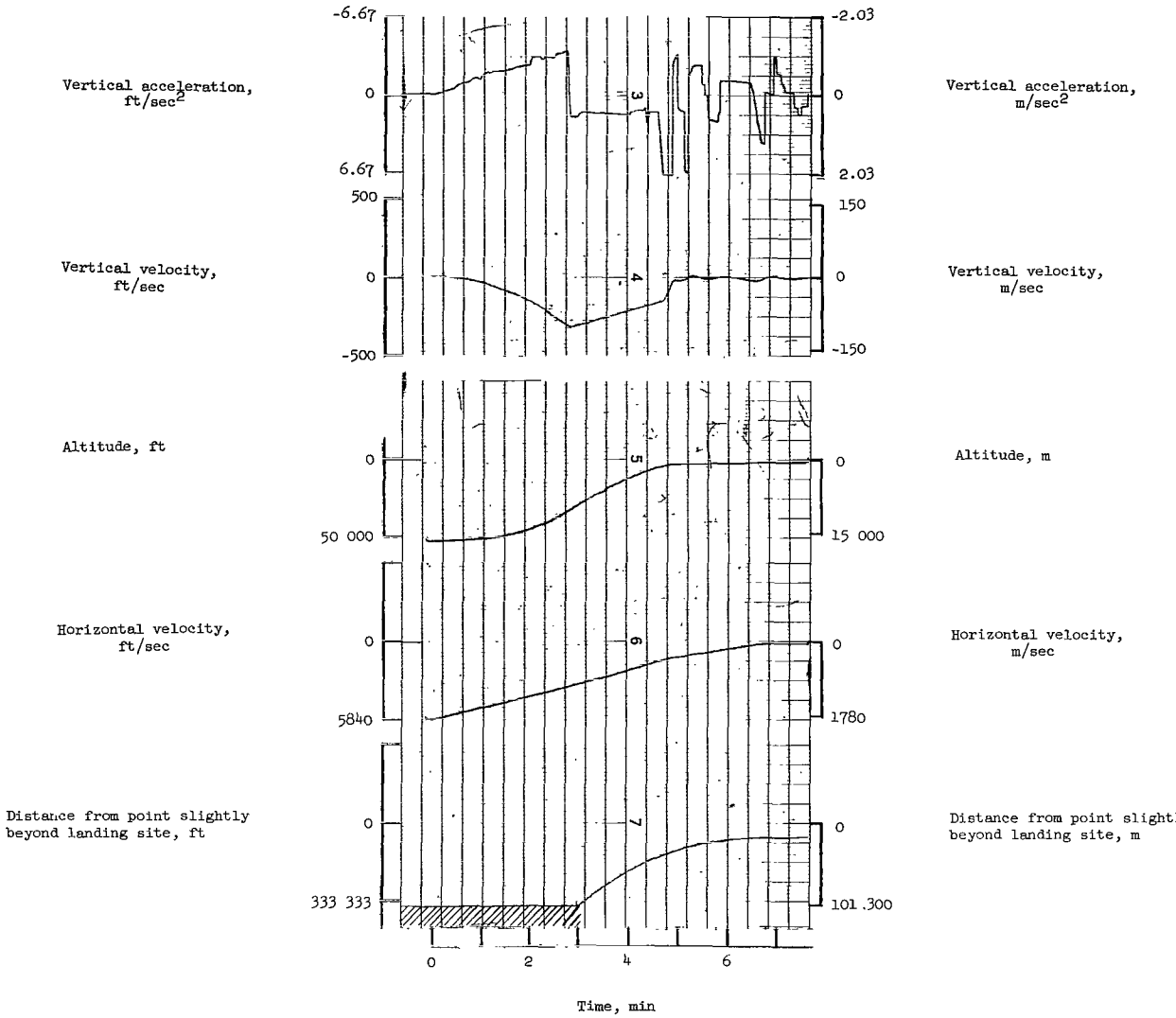

Figure 9.- Typical piloted lunar-letdown maneuver.

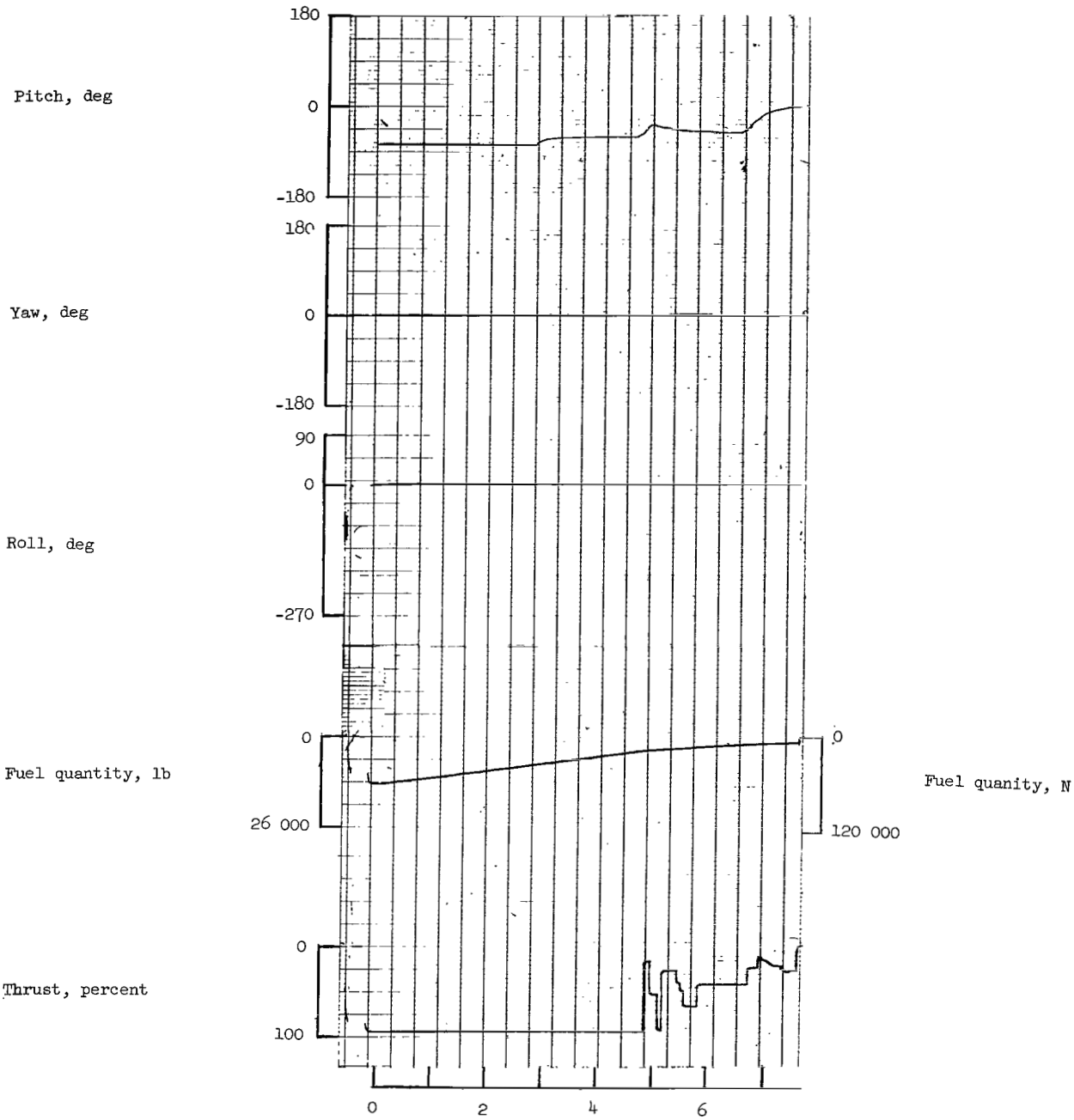

Figure 9.- Concluded.

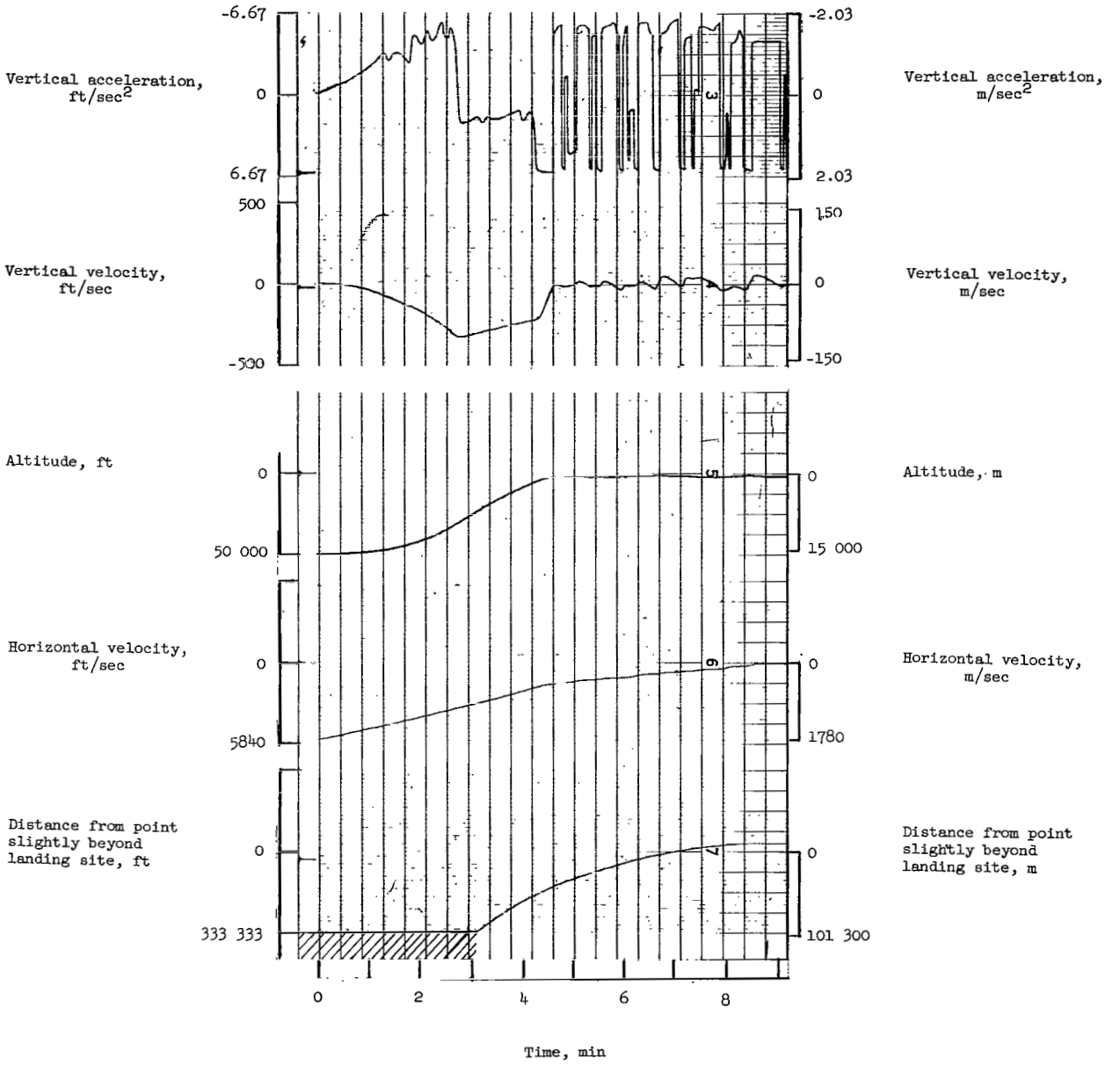

Figure 10.- Piloted lunar-letdown maneuver with all three attitude controls having damper failures.

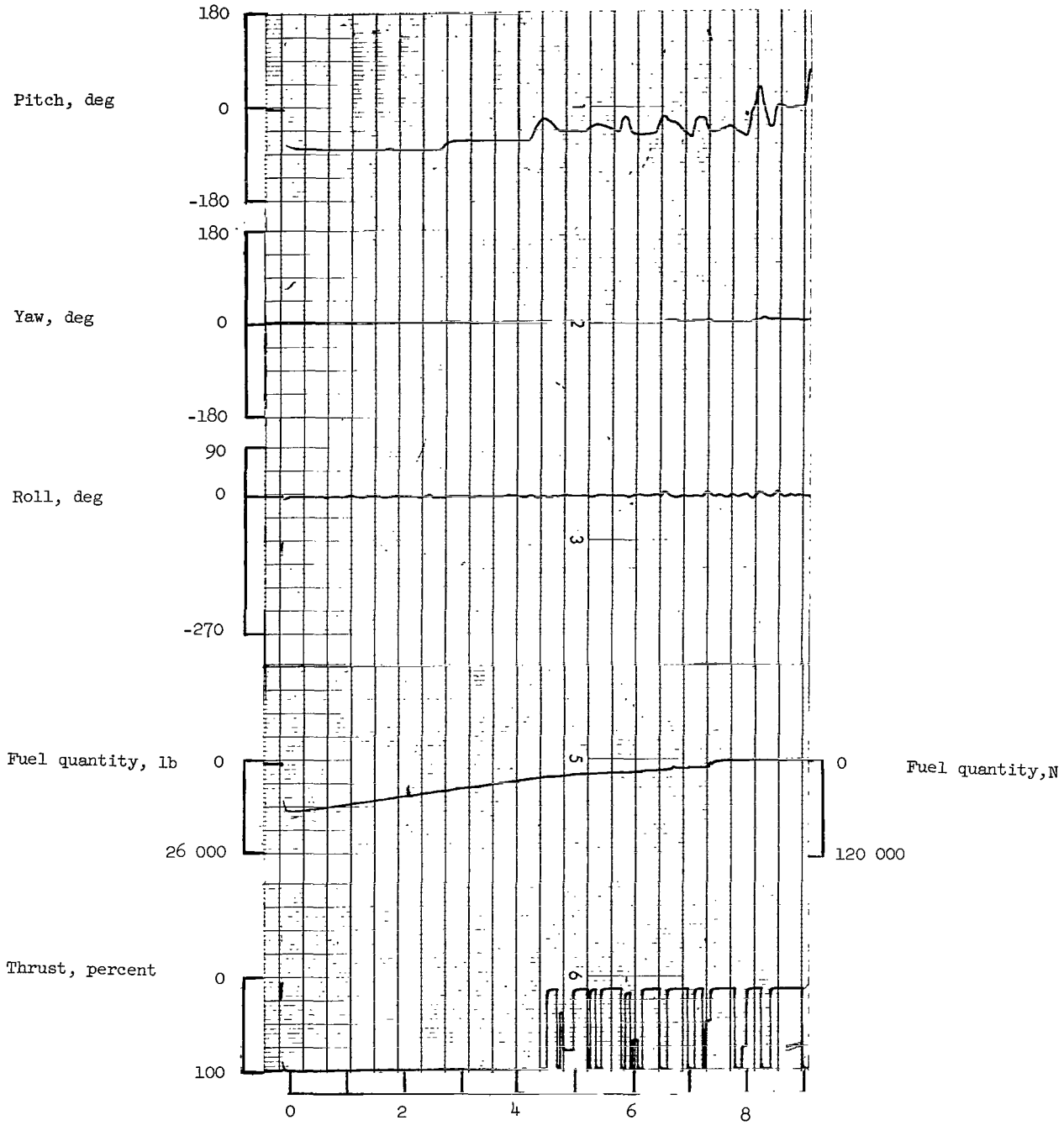

Figure 10.- Concluded.

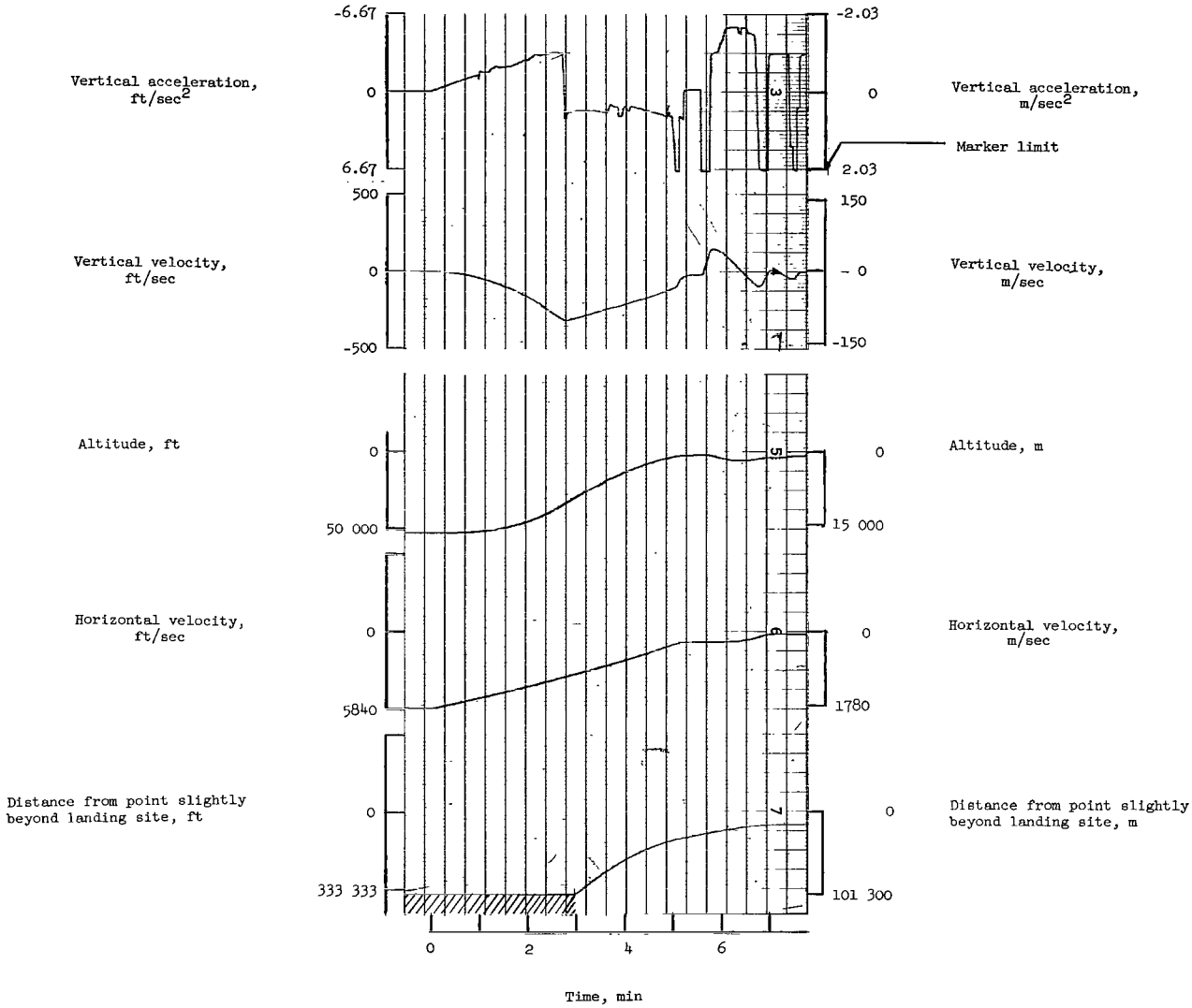

Figure 11.- Piloted lunar-letdown maneuver with the system-failures task added.

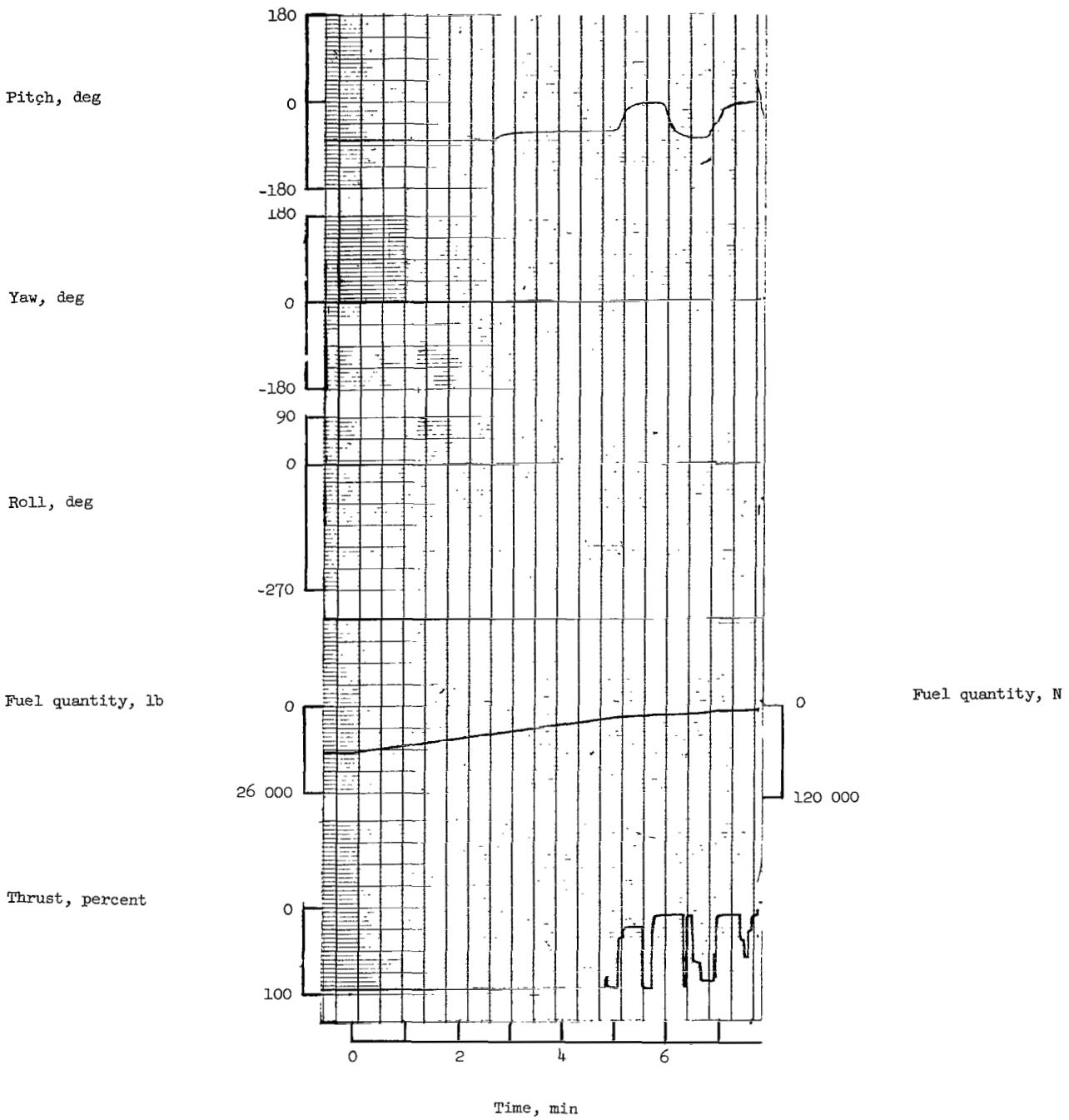

Figure 11.- Concluded.

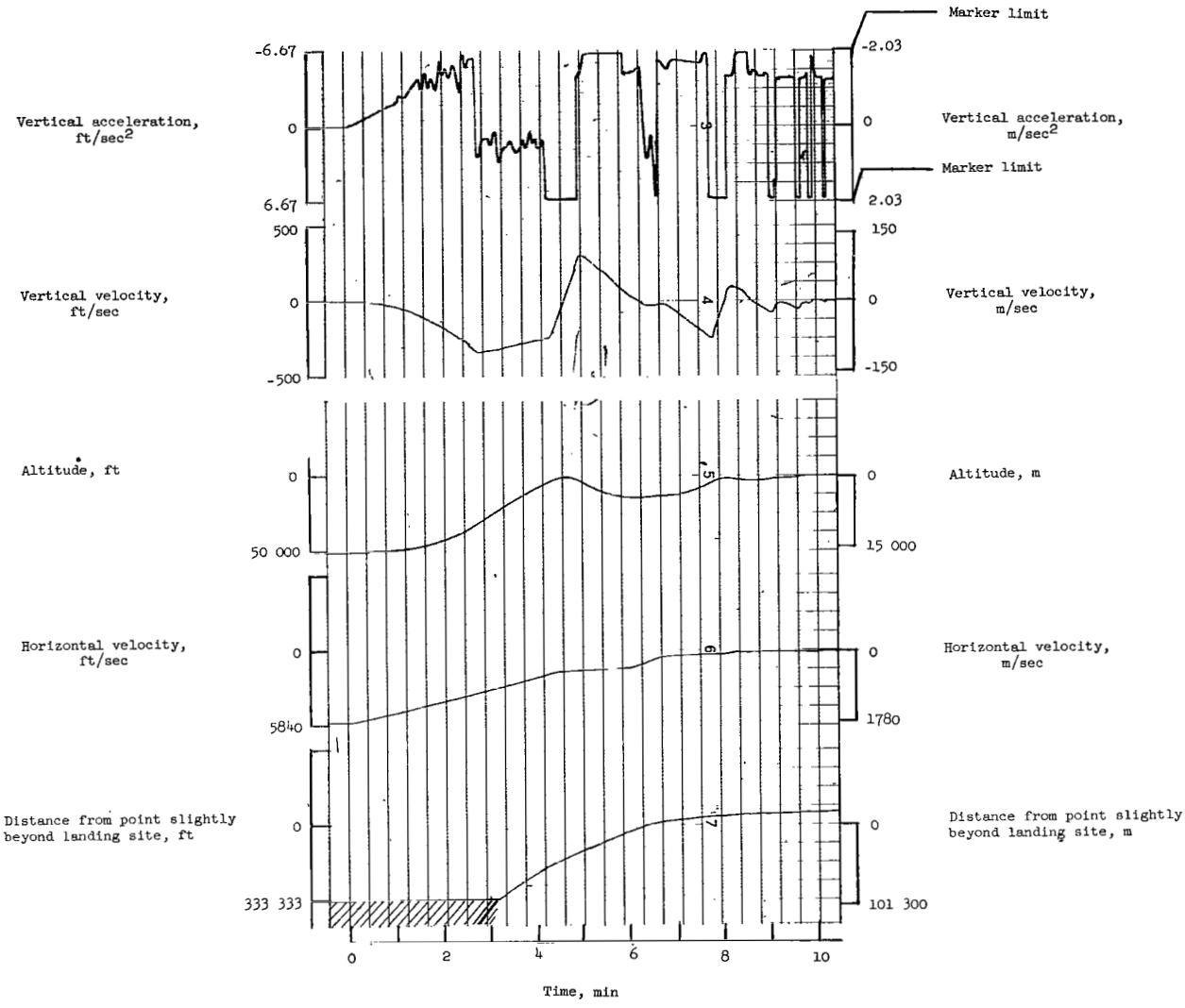

Figure 12.- Piloted lunar-letdown maneuver with all three attitude controls having damper failures and with the system-failures task added.

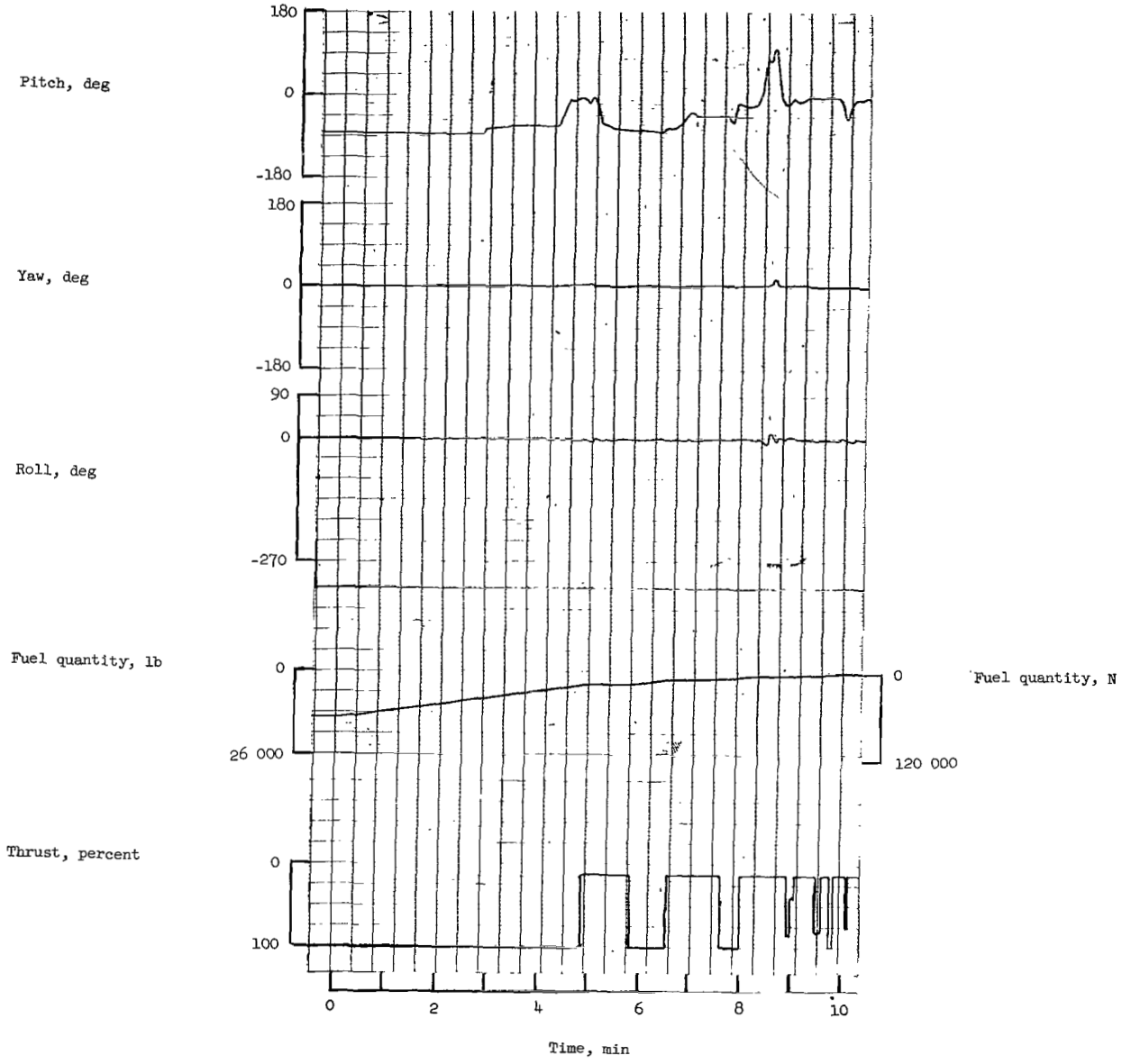

Figure 12.- Concluded.

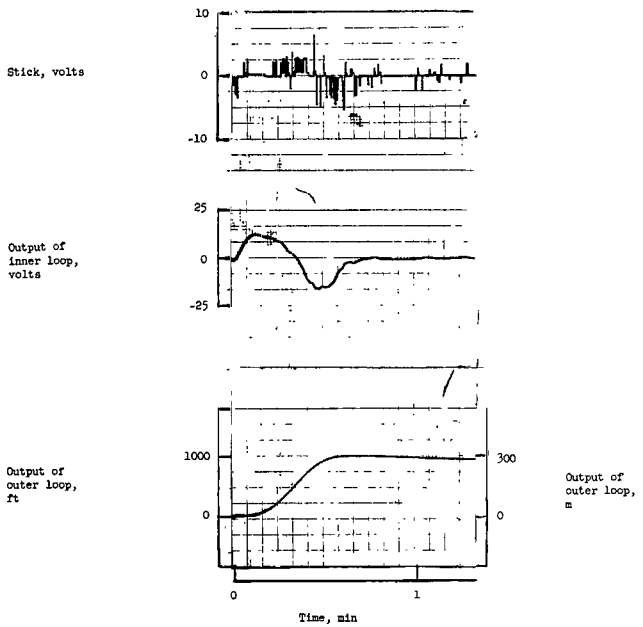

(a) Piloted maneuver.

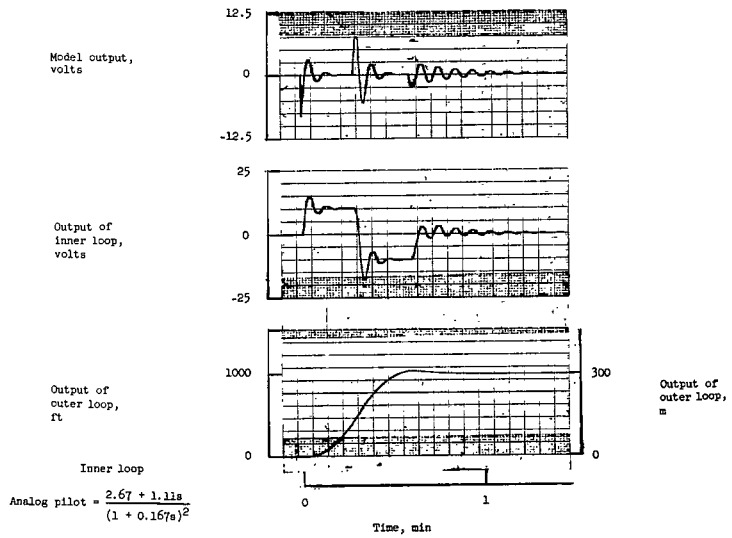

Inner loop

$$\text{Analog pilot} = \frac{2.67 + 1.11s}{(1 + 0.167s)^2}$$

$$\text{Dynamics} = \frac{0.5}{s(s + 0.5)}$$

Outer loop

$$\text{Analog pilot} = \frac{0.009 + 0.083s}{(1 + 0.1s)^2}$$

$$\text{Dynamics} = \frac{5.36}{s^2}$$

(b) Analytical representation of piloted maneuver.

Figure 13.- Comparison of pilot and model in a multiloop simulation.

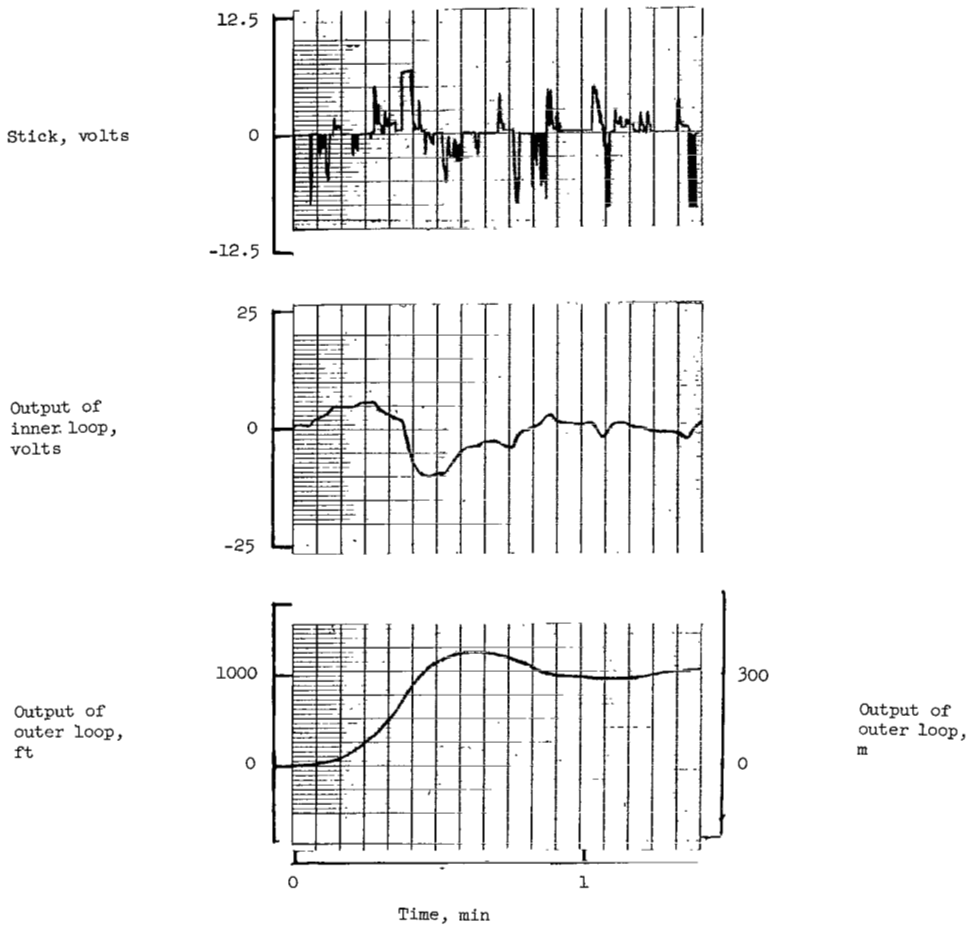

(a) Piloted maneuver.

Figure 14.- Comparison of pilot and models in a multiloop simulation with system failures as the side task.

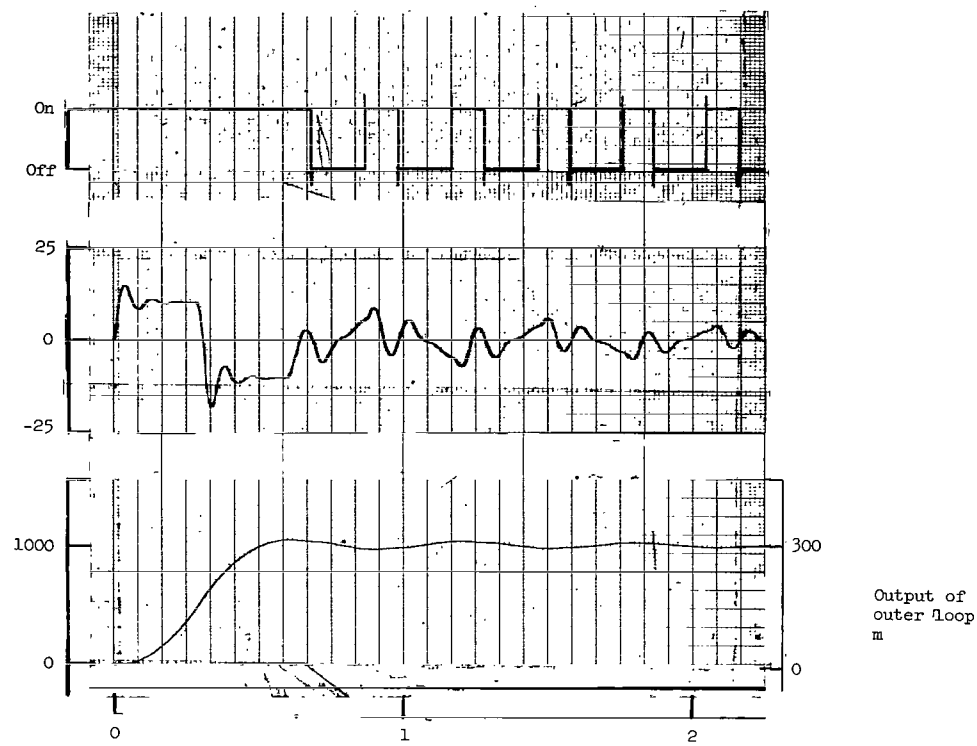

Inner loop

$$\text{Analog pilot} = \frac{2.67 + 1.11s}{(1 + 0.167s)^2}$$

$$\text{Dynamics} = \frac{0.5}{s(s + 0.5)}$$

Outer loop

$$\text{Analog pilot} = \frac{0.009 + 0.083s}{(1 + 0.1s)^2}$$

$$\text{Dynamics} = \frac{5.36}{s^2}$$

(b) Analytical representation of end portion of piloted maneuver.

Figure 14.- Continued.

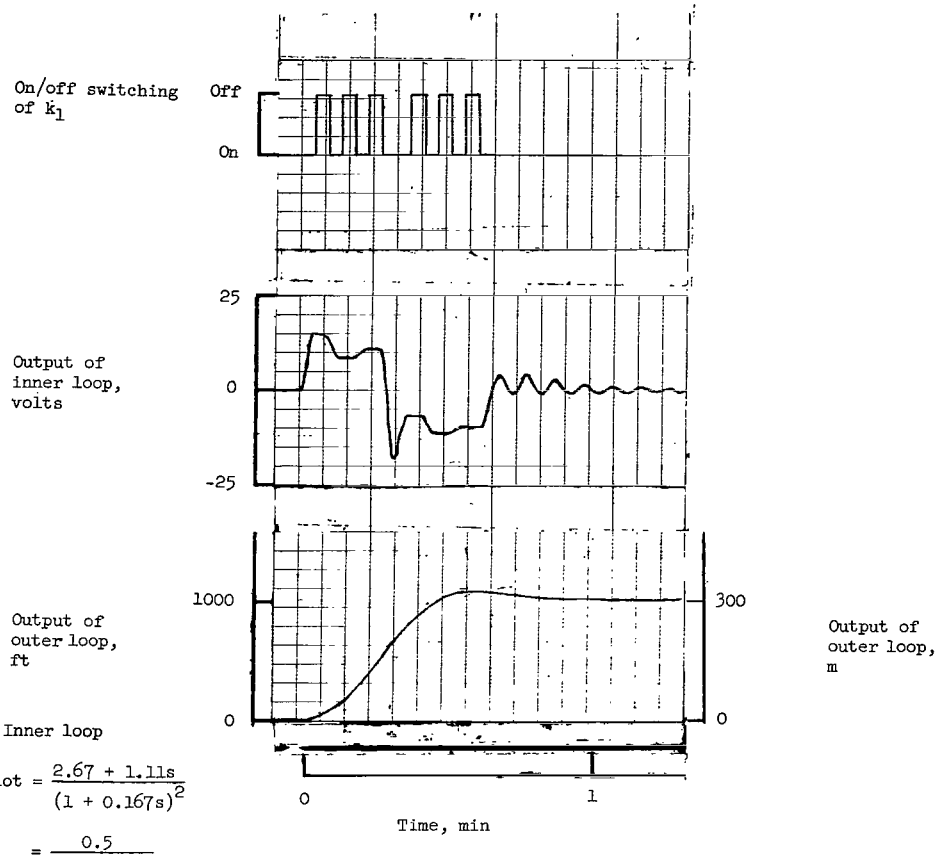

Inner loop

$$\text{Analog pilot} = \frac{2.67 + 1.11s}{(1 + 0.167s)^2}$$

$$\text{Dynamics} = \frac{0.5}{s(s + 0.5)}$$

Outer loop

$$\text{Analog pilot} = \frac{0.009 + 0.083s}{(1 + 0.1s)^2}$$

$$\text{Dynamics} = \frac{5.36}{s^2}$$

(c) Analytical representation of first portion of piloted maneuver.

Figure 14.- Concluded.

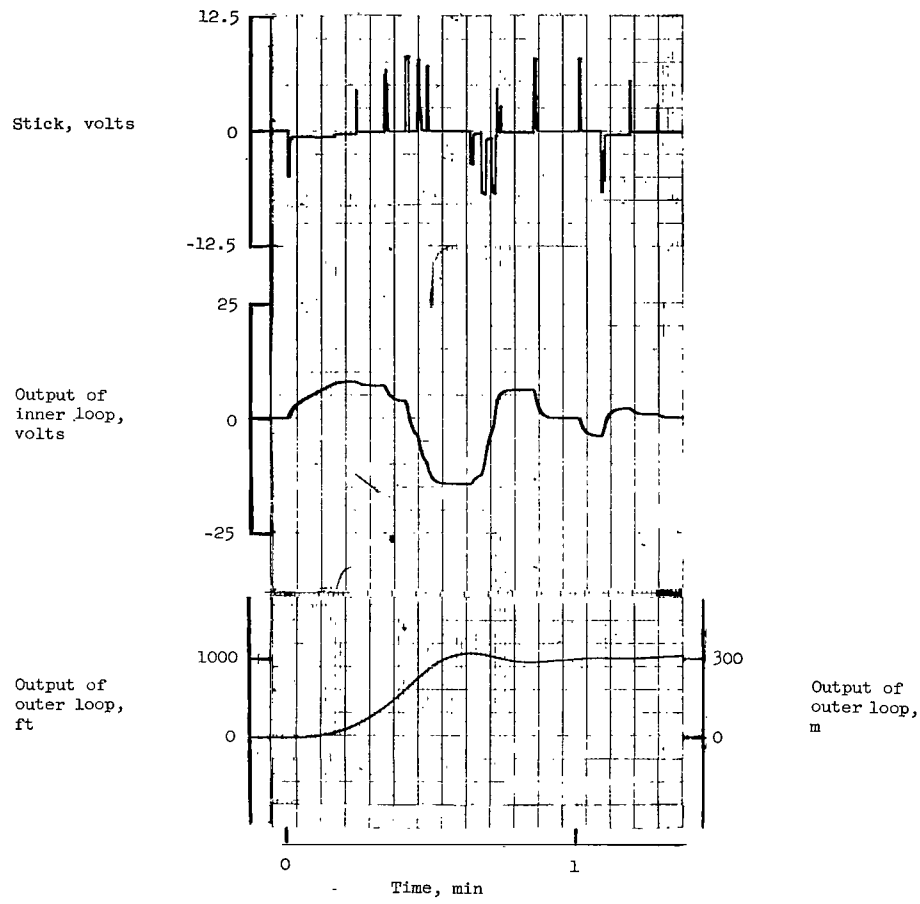

Figure 15.- Piloted multiloop maneuver with the motor response task being performed at 4.1 bits/sec.

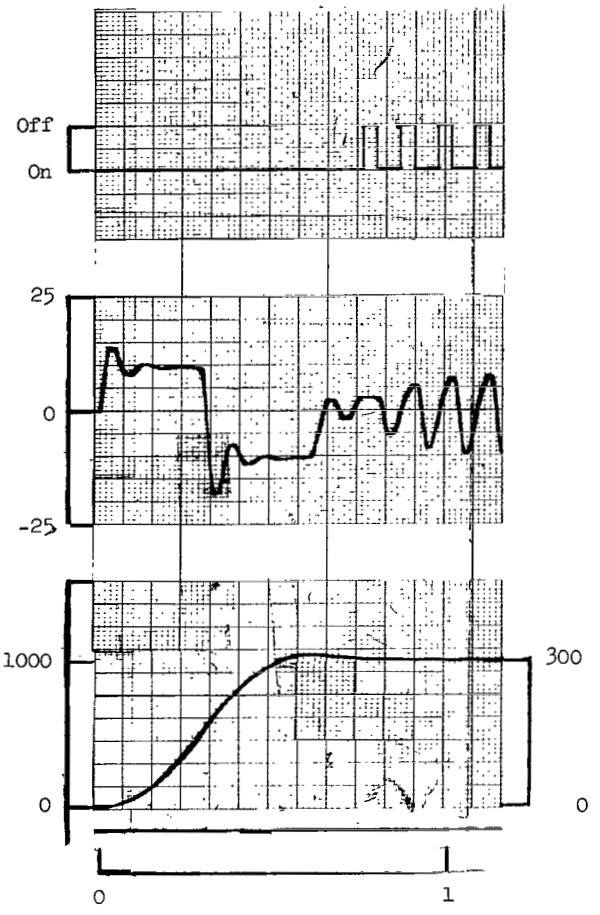

Inner loop

$$\text{Analog pilot} = \frac{2.67 + 1.11s}{(1 + 0.167s)^2}$$

$$\text{Dynamics} = \frac{0.5}{s(s + 0.5)}$$

Outer loop

$$\text{Analog pilot} = \frac{0.009 + 0.083s}{(1 + 0.1s)^2}$$

$$\text{Dynamics} = \frac{5.36}{s^2}$$

Figure 16.- Analytical representation of end portion of multiloop simulation with both the on and off times fixed.

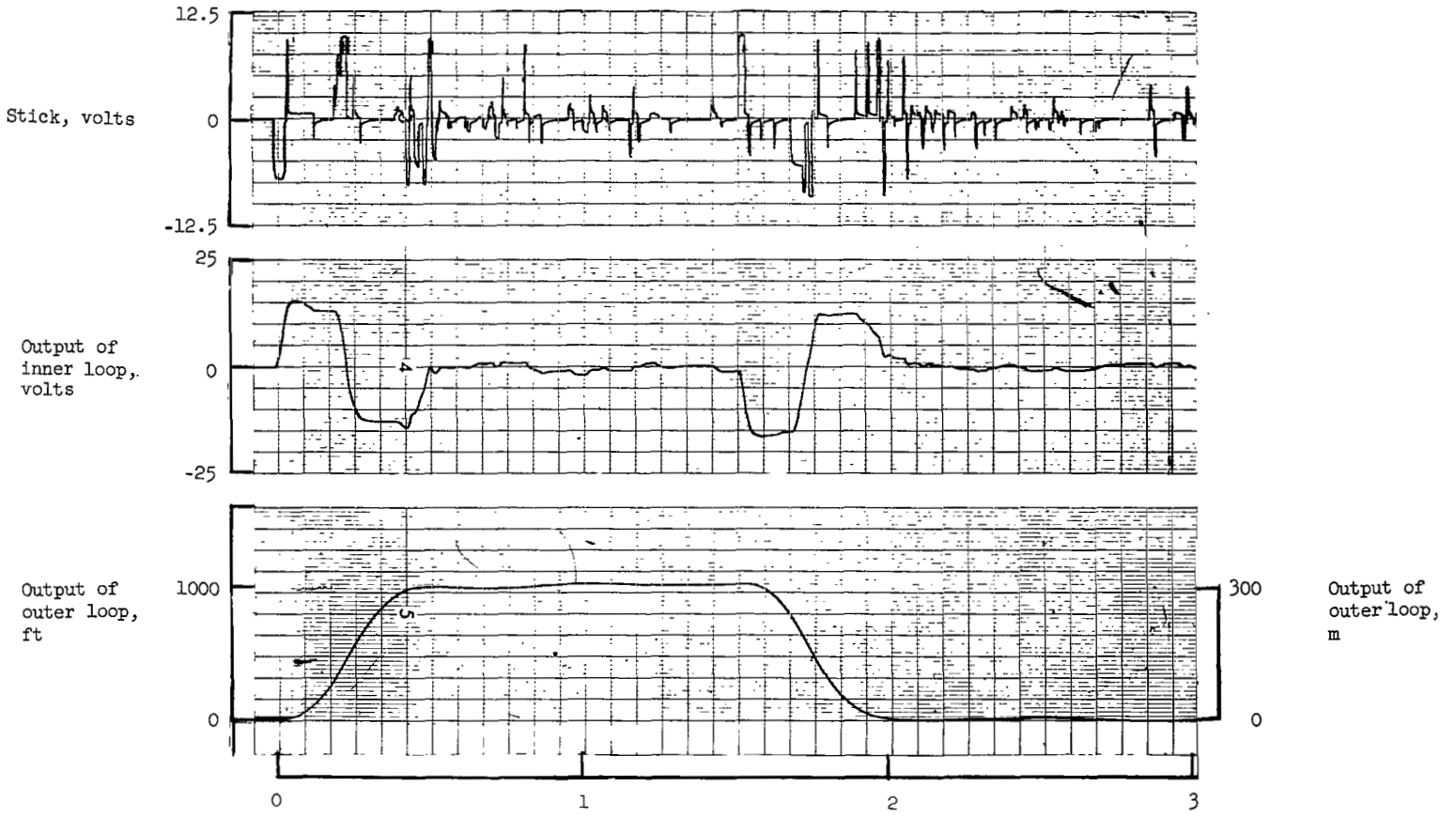

Figure 17.- Piloted multiloop simulation with no side tasks.

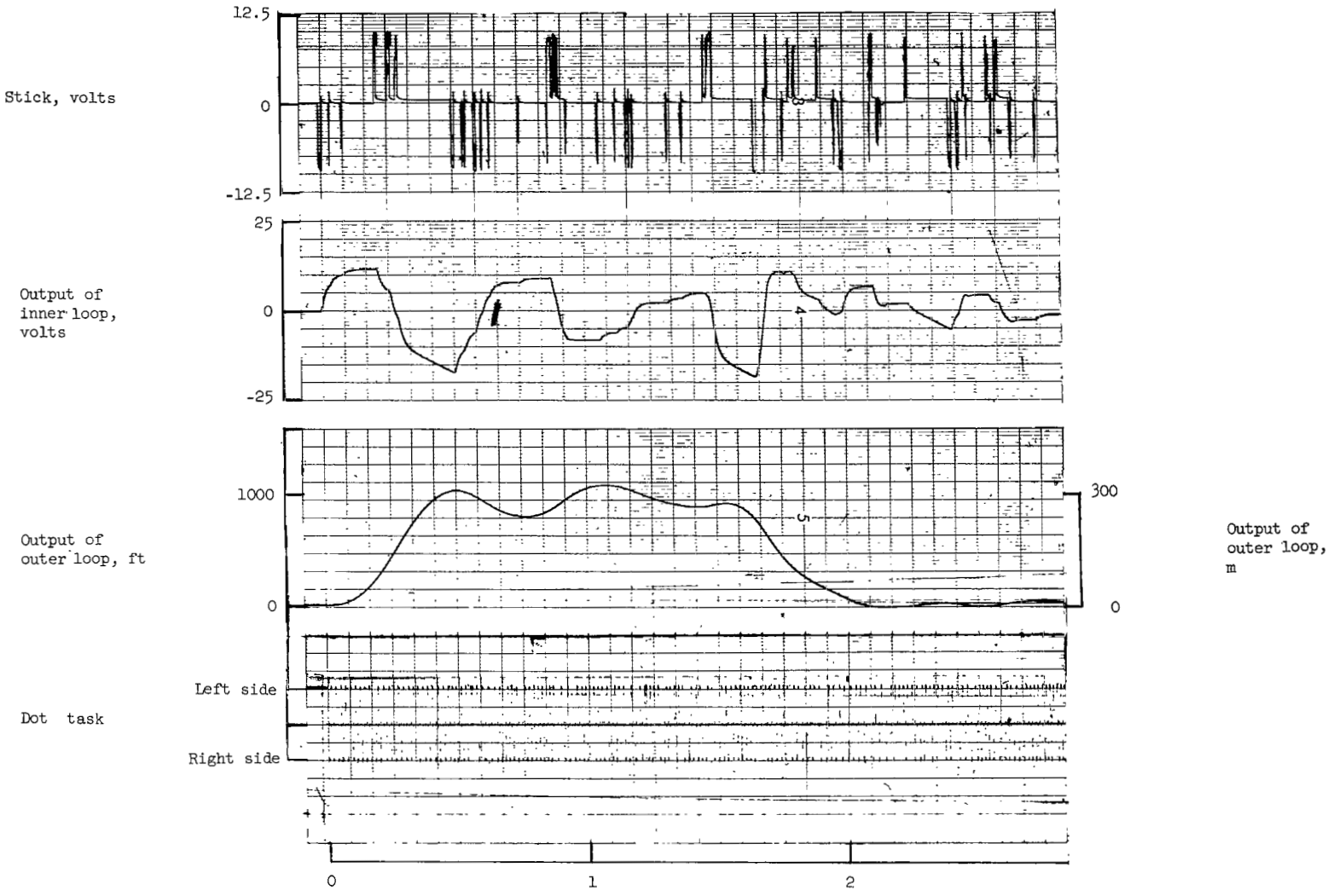

Figure 18.- Piloted multiloop simulation with motor response task being performed at 7.8 bits/sec.

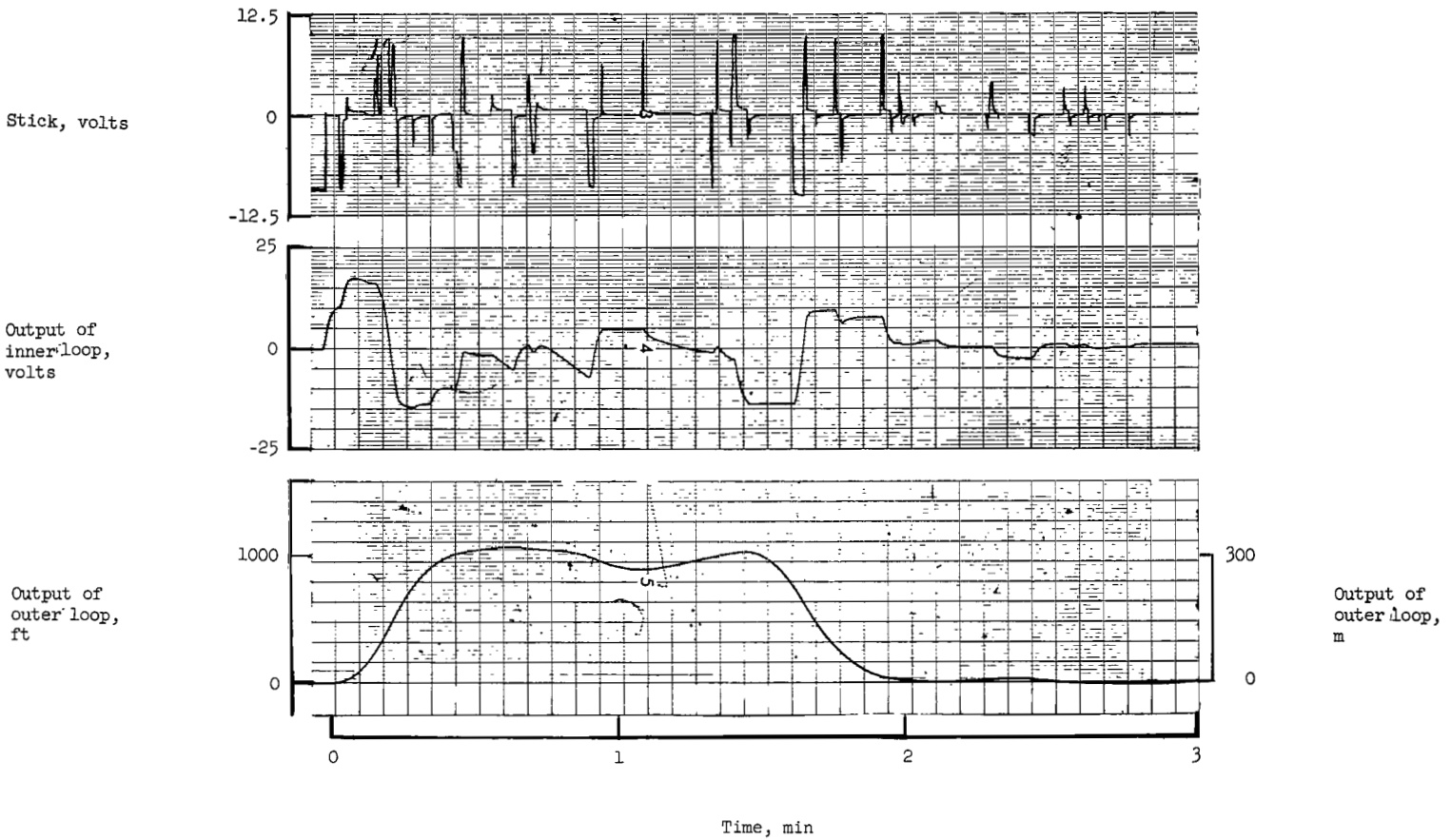

Figure 19.- Piloted multiloop simulation with system-failures task.

"The aeronautical and space activities of the United States shall be conducted so as to contribute . . . to the expansion of human knowledge of phenomena in the atmosphere and space. The Administration shall provide for the widest practicable and appropriate dissemination of information concerning its activities and the results thereof."

—NATIONAL AERONAUTICS AND SPACE ACT OF 1958

NASA SCIENTIFIC AND TECHNICAL PUBLICATIONS

TECHNICAL REPORTS: Scientific and technical information considered important, complete, and a lasting contribution to existing knowledge.

TECHNICAL NOTES: Information less broad in scope but nevertheless of importance as a contribution to existing knowledge.

TECHNICAL MEMORANDUMS: Information receiving limited distribution because of preliminary data, security classification, or other reasons.

CONTRACTOR REPORTS: Scientific and technical information generated under a NASA contract or grant and considered an important contribution to existing knowledge.

TECHNICAL TRANSLATIONS: Information published in a foreign language considered to merit NASA distribution in English.

SPECIAL PUBLICATIONS: Information derived from or of value to NASA activities. Publications include conference proceedings, monographs, data compilations, handbooks, sourcebooks, and special bibliographies.

TECHNOLOGY UTILIZATION PUBLICATIONS: Information on technology used by NASA that may be of particular interest in commercial and other non-aerospace applications. Publications include Tech Briefs, Technology Utilization Reports and Notes, and Technology Surveys.

Details on the availability of these publications may be obtained from:

SCIENTIFIC AND TECHNICAL INFORMATION DIVISION

NATIONAL AERONAUTICS AND SPACE ADMINISTRATION

Washington, D.C. 20546